Climate sensitivity from radiative-convective equilibrium: A chalkboard approach[a)]

Nadir Jeevanjee[b)]
Geophysical Fluid Dynamics Laboratory, Princeton, New Jersey 08540

(Received 22 November 2022; accepted 22 May 2023)

Simple models for Earth's climate sensitivity (i.e. its temperature response to radiative forcing) are developed by combining the time-tested idealization of one-dimensional radiative-convective equilibrium (RCE) with simple yet quantitatively reasonable models for CO_2 forcing and the water vapor feedback. Along the way, we introduce key paradigms including the emission level approximation, the forcing-feedback decomposition of climate sensitivity, and "Simpson's law" for water vapor thermal emission. We also discuss climate feedbacks unaccounted for in this RCE framework, as well as differing variants of climate sensitivity, all of which may be ripe for their own chalkboard treatments.
https://doi.org/10.1119/5.0135727

I. INTRODUCTION

Earth's equilibrium climate sensitivity (ECS), or the long-term global-mean surface temperature change due to a doubling of CO_2, is arguably the most central quantity in climate science. First studied by Arrhenius in 1896,[1] ECS sets the overall magnitude and, thus, the severity of global warming and remains a topic of intense interest to the present day.[2]

The consensus value of ECS has remained close to 3 K for decades, throughout many successive generations of model intercomparisons and literature reviews, most notably the assessment reports from the Intergovernmental Panel on Climate Change (IPCC).[3] These assessments have been based largely on calculations with numerical models of increasing complexity, along with observations and paleoclimate reconstructions. However, the first credible estimate of ECS, given by Manabe and Wetherald[4] in 1967 as 2–3 K, used a highly simplified one-dimensional representation of the climate system known as *radiative-convective equilibrium* (RCE; we refer to this paper hereafter as MW67). This model for Earth's climate makes some drastic simplifications, such as representing the atmosphere in terms of a single, global average column, but then treats other aspects of the climate system in detail, such as the frequency-dependent greenhouse gas radiative transfer of both water vapor (H_2O) and carbon dioxide (CO_2). These approximations, and insight they facilitated, have proved remarkably durable, and were recognized with Manabe's receipt of part of the 2021 Nobel Prize in Physics.[5]

The simplicity of Manabe's RCE approach and the robustness of the 3 K value for ECS suggest that much of the physics of ECS might actually be understood using a handful of basic physical principles, rather than lying hidden behind the intractable complexity of the climate system. Indeed, recent research has shown that essential topics, such as CO_2 radiative forcing[6] and the H_2O feedback,[7] can be described to a reasonable approximation with simplified models amenable to analytic description. Taken together, such models allow for an analytic estimate of ECS, at least within the simplified context of RCE. A self-contained formulation of such an estimate is a primary goal of this paper.[8]

The utility of such an estimate and the motivations for documenting it here are many-fold. The most obvious motivation is for classroom teaching. Current texts in climate science at the advanced undergraduate or beginning graduate level, such as the excellent books by Hartmann[9] and Pierrehumbert,[10] treat the fundamentals extremely well and use them to build intuition but then tend to jump to empirical observations and numerical simulations to describe real-world phenomena. This is often the best that can be done, but reasonably quantitative chalkboard estimates (where possible) help fill this gap between fundamental theory and empirical observation. Such back-of-the-envelope reasoning is also helpful for everyday practitioners trying to understand and debug the behavior of complex climate models.[11] The analytical approach taken here might also appeal more naturally to physicists, providing them a more suitable entry point for understanding or perhaps even contributing to climate science.

However, there are also more profound reasons for pursuing a simplified understanding of ECS and climate science more broadly.[12] Simple models of the kind developed here embody our understanding of the subject at its most basic level. This philosophy is well known to physicists in the guise of Fermi problems and the Feynman lectures. Given the societal importance of climate change, as well as lingering skepticism about it in some quarters, a chalkboard explanation of ECS, even if only approximate, seems essential for demonstrating the depth of our understanding.

Given this motivation, we develop an estimate of ECS in the simplified framework of RCE pioneered by Manabe. We begin by establishing the paradigm of radiative-convective equilibrium as well as the forcing-feedback framework. We then turn to simple models of the greenhouse effect for both CO_2 and H_2O, which lead to analytical descriptions of both CO_2 forcing and the water vapor feedback. These ingredients are then combined, via the forcing-feedback framework, to yield an analytical estimate of ECS. We will find that this estimate is around 2 K, within the range found by MW67 but somewhat smaller than the consensus value of 3 K. This discrepancy is due to the approximations inherent in the RCE approach, which neglects clouds and changes in absorbed solar radiation. We then discuss these phenomena and the prospects for capturing their effects via principled estimates. We close by introducing other metrics of climate sensitivity that account for ocean heat uptake and the carbon cycle, and for which a chalkboard understanding might also be useful.

For classroom instruction, this material might be considered a unit of perhaps eight lectures at the advanced undergraduate or beginning graduate level for either physics students or students of atmospheric and climate science. Suggestions for exercises are sprinkled throughout the main text and the endnotes.

II. RADIATIVE-CONVECTIVE EQUILIBRIUM (RCE)

We begin by building a very simple model for Earth's surface temperature T_s, based on the idea of radiative-convective equilibrium (RCE), which we explain in detail below. Before turning to RCE, however, we must consider the even more basic notion of planetary energy balance.

A. Planetary energy balance

The zeroth order determinant of T_s is the amount of sunlight Earth receives. The solar flux at Earth's orbit is $S_0 = 1360\,\mathrm{W/m^2}$, and this flux is incident on an effective surface area πR_E^2 (the projected area of the Earth onto a plane perpendicular to the Sun's rays, where R_E is Earth's radius). A significant fraction of this incident flux is reflected back to space, primarily via clouds and gaseous atmospheric (Rayleigh) scattering, as well as from bright surfaces such as deserts and ice caps. This fraction is known as Earth's *albedo* α, measured to be $\alpha \approx 0.30$.[13]

Dividing by the Earth's total surface area $4\pi R_E^2$ then gives the globally averaged net incoming solar radiation,

$$S \equiv \frac{S_0(1-\alpha)}{4} \approx 240\,\mathrm{W/m^2}. \tag{1}$$

The most basic physical constraint on climate is that of *planetary energy balance*, which says that in steady-state S must be balanced by outgoing thermal radiation, also known as the "outgoing longwave radiation," or OLR (here "longwave" means thermal infrared). We estimate OLR as blackbody emission,

$$\mathrm{OLR} = \sigma T_{\mathrm{em}}^4, \tag{2}$$

for some "emission temperature" T_{em}. Planetary energy balance then reads

$$S = \mathrm{OLR} \tag{3a}$$

$$= \sigma T_{\mathrm{em}}^4. \tag{3b}$$

The observed value of S yields $T_{\mathrm{em}} = 255$ K. This is much colder than the observed global average surface temperature $T_s = 288$ K but is a reasonable estimate of an effective *atmospheric* temperature, consistent with the fact that OLR largely emanates not from the surface, but from atmospheric greenhouse gases (GHGs, which are gases that absorb and emit thermal infrared radiation—most prominently water vapor and carbon dioxide). However, given the atmospheric T_{em}, how can we find T_s? How are surface and atmospheric temperatures related?

B. Single-layer radiative equilibrium

Perhaps the simplest model for estimating T_s in the presence of GHGs is that of a single-layer atmosphere of unit emissivity, i.e., one that absorbs and emits as a perfect blackbody, pictured on the left hand side of Fig. 1 (ignoring convective processes for the moment). Such an atmosphere is characterized by an atmospheric temperature T_a, blackbody emission $\sigma {T_a}^4$ from GHGs emanating both upwards to space and downwards to the surface, and transparency to sunlight.[14] The energy budgets at the top of the atmosphere (TOA) and surface then read (Fig. 1)

$$\mathrm{TOA}: S = \sigma {T_a}^4, \tag{4a}$$

$$\mathrm{surf}: S + \sigma {T_a}^4 = \sigma {T_s}^4. \tag{4b}$$

These equations can be immediately solved to yield $T_a = T_{\mathrm{em}} = 255$ K and $T_s = 2^{1/4} T_{\mathrm{em}} = 303$ K, overestimating T_s by 15 K.

Despite this disagreement, this model is standard in introductory texts.[15] Many of these texts remedy this disagreement by introducing a non-unit emissivity for the atmosphere, but the value of this emissivity is typically set by *requiring*

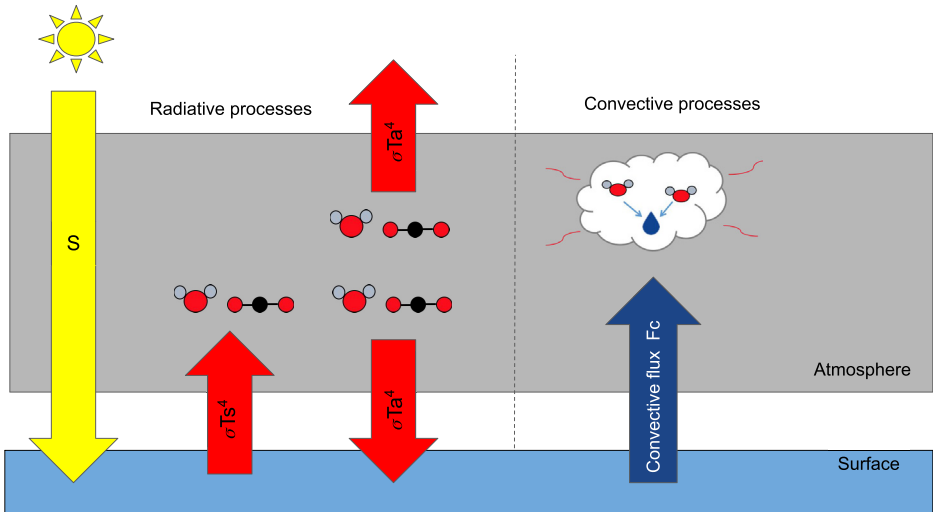

Fig. 1. A cartoon of radiative-convective equilibrium. See the text for explanation.

$T_s = 288$K, thus eliminating the model's predictive power. Furthermore, this approach does not remedy the model's grossest approximation, which is not that of unit emissivity but rather of neglecting heat transfer by *convection*.

C. A radiative-convective equilibrium model

Convection brings water vapor and heat from the surface into the interior of the atmosphere, where the water vapor condenses to form cloud and rain drops. This condensation releases the latent heat of vaporization which was drawn from the surface when the molecules first evaporated, and this heat from condensation is then radiated out to space by atmospheric GHGs, closing the loop. These processes are depicted on the right-hand side of Fig. 1. Thus, planetary energy balance is not achieved through purely radiative means but is mediated by convection, with water vapor as the key middleman. The atmosphere is, thus, better thought of as in a state of *radiative-convective equilibrium*, or RCE for short.[16]

To incorporate this into the simple one-layer model (4), we must add a convective heat flux F_c to the surface energy balance (4b). An additional variable requires an additional equation, however. To obtain this, we invoke the fact that convective heat fluxes are extremely efficient at transferring heat to the atmosphere, with two simplifying consequences: The surface temperature becomes essentially continuous with the atmospheric temperature near the surface, and atmospheric temperature profiles $T(z)$ lie more or less along a convective *adiabat*. A convective adiabat is the temperature profile of a parcel lifted adiabatically from the surface; such a parcel will expand and cool as it rises along the z-axis to lower pressures, much like the cool air escaping from the valve of a pressurized bicycle tire. For a dry air parcel, this profile is determined by the *dry adiabatic lapse rate*,

$$-\left.\frac{dT}{dz}\right|_{\text{dry}} = \frac{g}{C_p} = 10\,\text{K/km} \quad \text{(dry lapse rate)}, \tag{5}$$

where g is the gravitational acceleration and C_p is the specific heat of air (see Appendix A, which includes a derivation of Eq. (5) from undergraduate thermodynamics). Moisture, along with atmospheric dynamics besides convection, modifies this lapse rate somewhat and makes it variable over the globe, with a global average value of

$$\Gamma \equiv -\frac{dT}{dz} \approx 6.5\,\text{K/km} \quad \text{(avg. lapse rate)}. \tag{6}$$

If we then assume a mean pressure $p_a = 0.5$ atm for our single-layer atmosphere, corresponding to a height of $z_a \approx 5$ km (Fig. 2),[17] then Eq. (6) yields the *convective constraint*,

$$T_s - T_a = \Gamma z_a = 32.5\,\text{K}. \tag{7}$$

Our single-layer RCE model is then

$$S = \sigma T_a^{\,4}, \tag{8a}$$

$$S + \sigma T_a^{\,4} = \sigma T_s^{\,4} + F_c, \tag{8b}$$

$$T_s - T_a = \Gamma z_a. \tag{8c}$$

Solving these equations is again straightforward: Eq. (8a) again yields $T_a = T_{em}$, so then Eq. (8c) yields

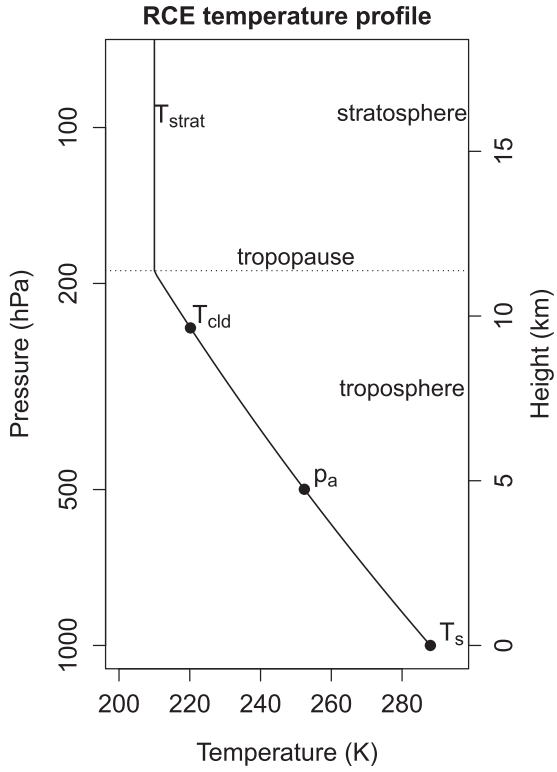

Fig. 2. A simplified RCE temperature profile, given by Eq. (10) with $T_s = 288$ K, along with an isothermal stratosphere with temperature $T_{strat} = 210$ K. The RCE profile (10) reaches up to the tropopause at roughly 12 km or 200 hPa, where it intersects the isothermal stratospheric profile. Also shown is the representative height of the single-layer atmosphere $p_a = 0.5$ atm $= 500$ hPa, as well as the characteristic cloud-top temperature $T_{cld} = 220$ K discussed in Sec. VI A.

$$T_s = T_{em} + \Gamma z_a = 287.5\,\text{K}. \tag{9}$$

This is remarkably close to the observed preindustrial value of 288 K. Furthermore, Eq. (9) tells us that this value stems from the radiative energy balance of the planet (as embodied in T_{em}), combined with the effects of convection on the temperature profile of the troposphere (as embodied in Γ). Thus, this single-layer RCE model appears to have significant pedagogical advantages over the single-layer radiative equilibrium model (4), but to our knowledge has not yet appeared in textbooks. It has appeared in the journal literature before, for instance, in the papers of Hansen *et al.*[18] and Payne *et al.*[19]

An important subtlety in the simple calculation above is that it was not necessary to solve the surface energy balance equation (8b); the convective flux F_c there acts as a Lagrange multiplier, taking on whatever value is required to satisfy Eq. (8b) subject to the constraint (8c); the convective flux is, thus, analogous to the tension in a pendulum arm, which takes on whatever value is required to satisfy Newton's laws while keeping the pendulum bob at a fixed distance from its origin.

While this simple one-layer RCE model yields a reasonable estimate of T_s and also illustrates the essence of how convection couples the surface and atmospheric temperatures, we will also need a vertically resolved view of the atmosphere for what follows. Figure 2 shows the following temperature profile, obtained by integrating Eq. (6) and also converting to pressure coordinates

$$T_a(z) = T_s - \Gamma z \tag{10a}$$

or

$$T_a(p) = T_s \left(\frac{p}{p_s}\right)^{R_d\Gamma/g}, \tag{10b}$$

where R_d is the gas constant for dry air and p_s is the surface pressure (see Appendix A for the definition of R_d and the derivation of Eq. (10b)). Equation (10a) is the vertically resolved version of the convective constraint Eq. (8c). In general, however, this convective constraint is only valid below an altitude of 10–15 km; this region is known as the *troposphere*. Above the troposphere lie the stratosphere and other air masses, which are heated primarily by ultraviolet solar absorption rather than convection, and are closer to radiative equilibrium rather than RCE. For simplicity, the stratosphere is represented here by an isothermal layer with characteristic temperature $T_{strat} = 210$ K, which is attached to the troposphere at the *tropopause*, where $T_a = T_{strat}$ (Fig. 2). The physics governing the height and temperature of the tropopause and, hence, the characteristic temperature T_{strat}, is still a subject of active research.[20]

A profound implication of the convective constraint (10a) is that the tropospheric temperature profile T_a is pegged to T_s, and the two cannot be varied independently. In other words, the surface and atmosphere should be thought of as a unit, with a single degree of freedom between them.[21] This tight surface-atmosphere coupling is a hallmark of RCE and has important consequences, as we will see below.

III. FORCING-FEEDBACK PRELIMINARIES

Now that we have a picture for Earth's energy flows and RCE, we can begin to think about climate sensitivity. An extremely useful paradigm for this is the *forcing-feedback framework*, which we describe next.

A. The forcing-feedback framework

In this paper, and in much (but certainly not all) climate modeling, the atmospheric CO_2 specific concentration[22] q (kg CO_2/kg air) is considered an *external* parameter, which is prescribed and does not respond to the internal dynamics of the system.[23] In studying changes in surface temperature ΔT_s, which result from changes in q, it turns out to be extremely convenient to decompose the system's response into two distinct processes, one which occurs at fixed T_s, and the other which occurs at fixed q.[24] (Also, it will be natural sometimes to use −OLR as our variable for planetary thermal energy flux, since an increase in −OLR indicates increasing planetary thermal energy.)

The first process is the decrease in OLR (increase in −OLR) due to an increase in q from an initial concentration q_i to a final concentration q_f, holding T_s fixed; since the lapse rate Γ does not depend on q, this also fixes $T_a(z)$ in Eq. (10a).[25] This decrease in OLR due to the change in q is known as the CO_2 *forcing*,

$$\mathcal{F} \equiv -(\mathrm{OLR}(q_f) - \mathrm{OLR}(q_i)) \tag{11}$$

($\mathcal{F}$ is the change in −OLR, so $\mathcal{F} > 0$ for a CO_2 increase). The forcing $\mathcal{F}$ breaks the planetary energy balance, causing additional heat to accumulate in the system.

Next, this heat accumulation causes a temperature increase ΔT_s and, hence, a countervailing *increase* in OLR (decrease in −OLR), which persists until the planetary energy balance (3a) is restored and a new equilibrium is established (how long this takes, and what happens along the way, is addressed in Sec. VII A). This increase in OLR due to increasing T_s can be approximated as $(d\mathrm{OLR}/dT_s)\Delta T_s$, where the derivative is taken at fixed $q = q_f$. Consistent with the sign convention in Eq. (11), we then define the "feedback parameter" λ as minus this derivative[26]

$$\lambda \equiv -\left.\frac{d\mathrm{OLR}}{dT_s}\right|_{q=q_f}. \tag{12}$$

Noting that $(d\mathrm{OLR}/dT_s)\Delta T_s = \mathcal{F}$ in equilibrium, we have $\Delta T_s = -\mathcal{F}/\lambda$. When $q_f = 2q_i$, we write the forcing as $\mathcal{F}_{2\times}$, and the corresponding ΔT_s is defined to be the *equilibrium climate sensitivity* (ECS), that is

$$\mathrm{ECS} = -\frac{\mathcal{F}_{2\times}}{\lambda}. \tag{13}$$

(The choice of a multiplicative rather than additive change in q for defining ECS will be discussed below.) Equation (13) is known as the *forcing-feedback* decomposition of ECS. It allows us to study ECS by studying $\mathcal{F}$ and λ separately, which we will do in Secs. IV and V, respectively. Note that we have ignored the possibility that the absorbed solar radiation S may also depend on T_s, which would contribute a dS/dT_s term to the definition of λ. We discuss these so-called "shortwave" feedbacks in Sec. VI.

B. Blackbody estimate of ECS

As an exercise, we will use Eq. (13) to estimate ECS using the blackbody approximation (2). The blackbody approximation allows us to calculate λ, but we still need a value for the forcing $\mathcal{F}_{2\times}$. For the moment, we obtain this by appealing to comprehensive radiative transfer calculations, which for decades[27] have found a fairly consistent value of

$$\mathcal{F}_{2\times} \approx 4\,\mathrm{W/m^2}. \tag{14}$$

We will provide a theoretical estimate of this number in Sec. IV.

Turning now to the feedback parameter λ, a blackbody estimate for this can be obtained from Eq. (2), noting also that T_{em} and T_s vary in a 1–1 fashion according to Eq. (9). Recalling that $T_{em} = 255$ K, this yields

$$\lambda_{\mathrm{blackbody}} = -\frac{d\mathrm{OLR}}{dT_s} = -4\sigma T_{em}^3 \approx -3.75\,\mathrm{W/m^2/K}. \tag{15}$$

According to Eq. (13), this yields $\mathrm{ECS} = (4\,\mathrm{W/m^2})/(3.75\,\mathrm{W/m^2/K}) \approx 1$ K, three times smaller than the consensus value of 3 K.

To understand why $\mathcal{F}_{2\times} \approx 4\,\mathrm{W/m^2}$, as well as make a better estimate of λ and hence ECS, we need to move beyond the blackbody approximation and account for the *spectral* nature of Earth's greenhouse effect, i.e., that the emission temperature T_{em} of outgoing longwave radiation actually depends rather markedly on frequency, and that T_{em} at a given frequency and T_s may not necessarily exhibit a 1–1 relationship as in Eq. (9). A key ingredient in understanding

how these quantities do behave will be the *emission level approximation*, which we turn to next.

C. Emission level approximation

In Sec. II, we defined Earth's emission temperature T_{em} in Eq. (2) and then assumed an average blackbody emission level $p_{\text{a}} = 0.5$ atm. This led to a 1–1 relationship between T_{em} and T_{s}, which allowed us to estimate λ.

To refine this, we first define a spectrally resolved emission temperature $T_{\text{em}}(\nu)$ by the relation,

$$\text{OLR}_\nu = \pi B(\nu, T_{\text{em}}(\nu)), \tag{16}$$

where OLR_ν is the spectrally resolved OLR in units of $\text{W}/(\text{m}^2 \cdot \text{cm}^{-1})$ and satisfying $\text{OLR} = \int \text{OLR}_\nu d\nu$, and $B(\nu, T)$ is the Planck density in units of $\text{W}/(\text{m}^2 \cdot \text{cm}^{-1} \cdot \text{sr})$. (The factor of π above accounts for integration over solid angle.)[28] The spectral coordinate here is "wavenumber" ν, defined as inverse wavelength and, thus, proportional to frequency, with standard unit of cm^{-1}. The definition (16) of $T_{\text{em}}(\nu)$, as the temperature whose Planck emission yields OLR_ν, straightforwardly generalizes the blackbody definition (2).

The next task is to determine what level(s) in the atmosphere determine $T_{\text{em}}(\nu)$, for a given ν. This task is aided by the following heuristic, illustrated in Fig. 3. Consider an atmospheric column with GHG molecules whose density ρ_{GHG} $[(\text{kg GHG})/\text{m}^3]$ decreases exponentially with height; this is true for both CO_2 and H_2O.[29] Now consider the emission to space (i.e., the contribution to the OLR_ν at a given ν) from these molecules, as pictured in Fig. 3. The top two layers (Fig. 3(a)) have little difficulty emitting to space, because their view is unobstructed, but the density of emitters in these layers is relatively low, so the emission will also be low. In the third layer (Fig. 3(b)), the molecules' view of space is still unobstructed (just barely), and their density is higher, so their emission to space is higher. For layers four and five (Fig. 3(c)), there are plenty of emitters, but their view is almost totally obstructed, so their emission to space is again very low. Thus, emission to space is maximized around a "sweet spot" where the absorbers/emitters above have not yet totally obstructed the view of space, but the density is high enough for emission to be appreciable. This sweet spot will be our emission level.

To formalize this, we need the notion of *optical depth*, defined as[30]

$$\tau_\nu(z) \equiv \int_z^\infty \underbrace{\kappa_{\text{ref}}(\nu)\frac{p}{p_{\text{ref}}}}_{(\text{m}^2/\text{kg})} \underbrace{\rho_{\text{GHG}}\, dz'}_{(\text{kg}/\text{m}^2)} = \frac{\text{Effective area of absorbers}}{\text{Actual area of column}}. \tag{17}$$

Here, $\kappa_{\text{ref}}(\nu)$ are the *mass absorption coefficients* of our GHG, which give the effective cross-sectional area of our GHG molecules at wavenumber ν per unit mass (units m^2/kg), evaluated at a reference pressure p_{ref}. This effective cross-section depends strongly on frequency (e.g., Figs. 4(a) and 5(a) below) but also scales with pressure approximately as p/p_{ref}, hence the presence of this factor in Eq. (17).[31] The factor of $\rho_{\text{GHG}}dz'$ in the integrand in Eq. (17) gives the absorber mass per unit area (kg/m^2) in an atmospheric layer of differential depth dz'. Thus, the integral τ_ν in Eq. (17) can be interpreted as the ratio of the integrated effective area of absorbers above height z to the actual area of the column, as noted in Eq. (17). Applying this notion to Fig. 3, we see that the top two layers with low emissions correspond to $\tau_\nu < 1$, where the total effective area of absorbers above is less than the actual area of the column (the "optically thin" regime). Similarly, the bottom two layers with low emissions correspond to $\tau_\nu > 1$, where the total effective area of absorbers above is greater than the actual area of the column (the "optically thick" regime). The sweet spot occurs around $\tau_\nu \approx 1$.

For simplicity, we further assume that *all* emission occurs at exactly $\tau_\nu = 1$; we refer to this as the *emission level approximation*.[32] With this in mind, we define our emission pressure $p_{\text{em}}(\nu)$ by the relation

$$\tau_\nu(p_{\text{em}}(\nu)) = 1. \tag{18}$$

This equation will form the basis for reasoning about both CO_2 forcing as well as the H_2O feedback, which are the subjects of Secs. IV and V.

IV. CO_2 FORCING

This section constructs a simple analytic model for the CO_2 forcing Eq. (11), with the aim of enabling a back-of-the-envelope estimate of the characteristic $4\,\text{W}/\text{m}^2$ value for $\mathcal{F}_{2\times}$.

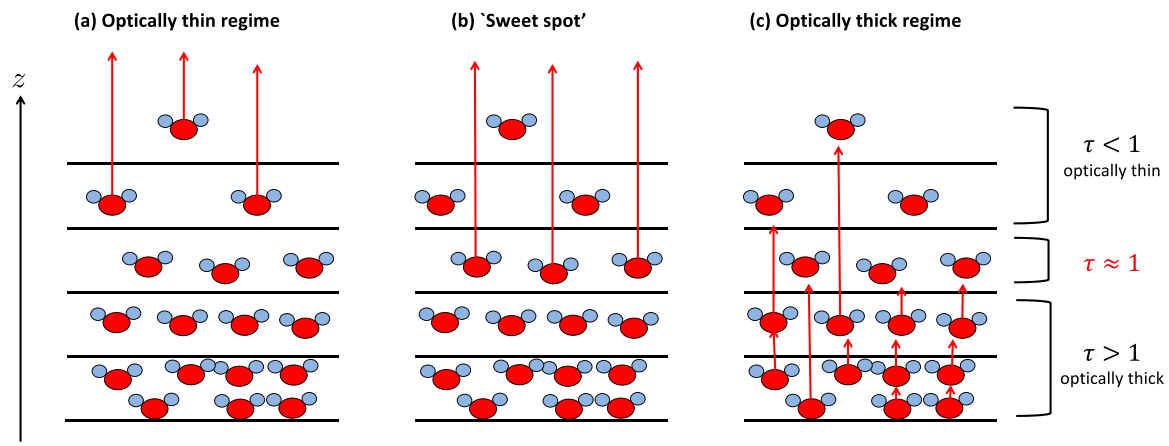

Fig. 3. Cartoon of emission to space from different atmospheric layers corresponding to different optical depths. Layer-wise emission to space maximizes at a sweet spot where the optical depth $\tau \approx 1$.

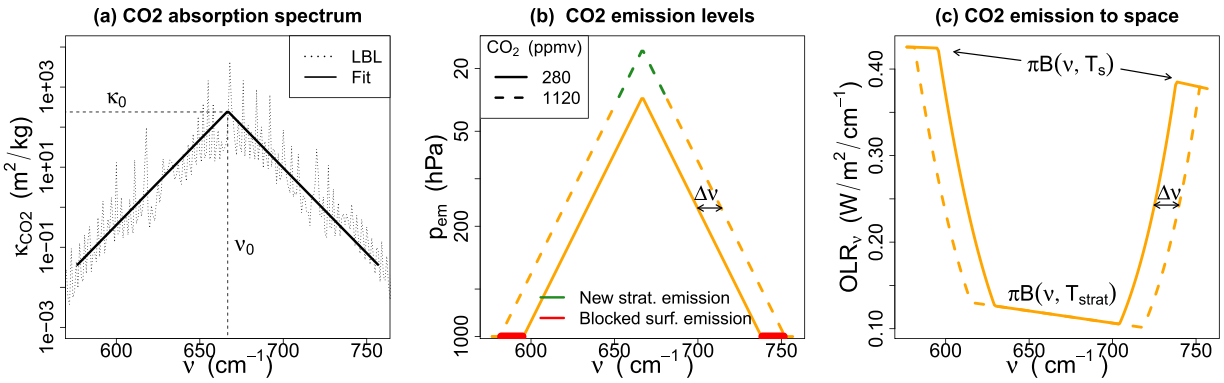

Fig. 4. (a) CO_2 absorption coefficients κ_{CO_2} as calculated[87] by a line-by-line (LBL) benchmark radiation code, coarse-grained into $10\,\mathrm{cm}^{-1}$ bins, along with an exponential fit of the form (19) with $\kappa_0 = 240\,\mathrm{m}^2/\mathrm{kg}$ and $l = 10.2\,\mathrm{cm}^{-1}$. Reference pressure and temperature for κ_{CO_2} are $(p_{\mathrm{ref}}, T_{\mathrm{ref}}) = (500\,\mathrm{hPa}, 260\,\mathrm{K})$. (b) Graph of emission levels p_{em} from Eq. (21), for CO_2 concentrations of 280 and 1120 ppm. (c) Graph of OLR_ν calculated as $\pi B(\nu, T(p_{\mathrm{em}}(\nu)))$, using the RCE temperature profile from Fig. 2.

The approach here is to consider spectral variations in CO_2 absorption but to do so in a simplified manner, so as to keep the model analytically tractable. The model we construct has precedent in relatively recent literature, e.g., the works of Wilson and Gea-Banacloche,[33] Seeley[34] Jeevanjee *et al.*,[35] and Romps *et al.*,[36] but has not yet appeared in textbooks. We present here a very simple version of the model, which can be generalized to include the effects of a non-isothermal stratosphere as well as spectral overlap between CO_2 and H_2O absorption.[37]

We begin with CO_2 reference mass absorption coefficients κ_{CO_2} in the strongly absorbing and climatically relevant $\nu 2$ bending mode centered on wavenumber $\nu_0 = 667\,\mathrm{cm}^{-1}$. Figure 4(a) displays this absorption spectrum.[38] A key simplification we make is to ignore fine-scale spectral structure and note that on a broad scale, $\kappa_{CO_2}(\nu)$ may be parameterized as

$$\kappa_{CO_2}(\nu) = \kappa_0 \exp\left(-\frac{|\nu - \nu_0|}{l}\right), \tag{19}$$

where κ_0 represents a smoothed peak absorption coefficient and l is a "spectroscopic slope," which sets the rate at which absorption declines away from the peak.

With Eq. (19) in hand, we next evaluate the optical depth integral (17) for CO_2, for which $\rho_{\mathrm{GHG}} = q\rho$ where q is a constant CO_2 specific concentration and ρ is the density of air. Plugging this into Eq. (17) and invoking hydrostatic balance $dp/dz = -\rho g$ [see also Eq. (A3)] then yields

$$\tau_{CO_2}(\nu, p) = \kappa_{CO_2}(\nu) \int_0^p \frac{p'}{p_{\mathrm{ref}}} \frac{q\,dp'}{g} = \frac{\kappa_{CO_2}(\nu) q}{2g} \frac{p^2}{p_{\mathrm{ref}}}. \tag{20}$$

The pressure broadening factor in the integrand above, as well as the fact that the mass of CO_2 in a layer is given by qdp'/g, conspire to give $\tau \sim p^2$.

Invoking the emission level approximation (18), as well as the "exponential spectroscopy" (19), we can set $\tau_{CO_2} = 1$ and invert Eq. (20) to find the emission levels $p_{\mathrm{em}}(\nu)$,

$$p_{\mathrm{em}}(\nu) = \sqrt{\frac{2gp_{\mathrm{ref}}}{q\kappa_0}} \exp\left(-\frac{|\nu - \nu_0|}{2l}\right). \tag{21}$$

These emissions levels are shown in Fig. 4(b) for $(q_{\mathrm{i}}, q_{\mathrm{f}}) = (280, 1120)$ ppm. (A quadrupling of CO_2 is easier to visualize than a doubling.) The p_{em} curves take the form of "emission triangles," which widen and deepen with increased CO_2. The red and green highlighted regions show that an increase in q yields a decrease in surface emission, as well as "new" emission from portions of the stratosphere (around 20 hPa) that were not emitting significantly before. Also, from Eq. (21) one can deduce that the change in width of the emission triangles with q is given by

$$\Delta\nu = l \ln\left(\frac{q_{\mathrm{f}}}{q_{\mathrm{i}}}\right). \tag{22}$$

Note the logarithmic dependence on q, which we comment on further below.

To turn this insight into a formula for CO_2 forcing, Fig. 4(c) shows $\mathrm{OLR}_\nu = \pi B(\nu, T_{\mathrm{em}})$ obtained by inserting the emission levels p_{em} from Fig. 4(b) into the temperature profile Eq. (10b) and then applying the Planck function. The large values on the outside of the CO_2 band correspond to surface emission $\pi B(\nu, T_{\mathrm{s}})$, and the smaller values in the center correspond to stratospheric emission $\pi B(\nu, T_{\mathrm{strat}})$ (i.e., where $p_{\mathrm{em}}(\nu) \lesssim 200\,\mathrm{hPa}$). Given the definition Eq. (11) of the forcing and the expression (22) for $\Delta\nu$, the forcing can then be read off from Fig. 4(c) as just the difference in the area under the solid and dashed curves, i.e.,

$$\mathcal{F} = 2l \ln\left(\frac{q_{\mathrm{f}}}{q_{\mathrm{i}}}\right) [\,\pi B(\nu_0, T_{\mathrm{s}}) - \pi B(\nu_0, T_{\mathrm{strat}})\,]. \tag{23}$$

This formula can also be interpreted via Fig. 4(b) as a swap of stratospheric emission for surface emission over spectral regions of total width $2\Delta\nu$. For an analytical derivation of Eq. (23), see Appendix B.

We are now in a position to make a back-of-the-envelope estimate of CO_2 forcing. Evaluating Eq. (23) for $T_{\mathrm{s}} = 288$ K, $T_{\mathrm{strat}} = 210$ K, and for $q_{\mathrm{f}} = 2q_{\mathrm{i}}$ yields the estimate

$$\begin{aligned}\mathcal{F}_{2\times} &\approx 2l \ln 2\,[\,\pi B(\nu_0, 288\,\mathrm{K}) - \pi B(\nu_0, 210\,\mathrm{K})] \\ &\approx 4.15\,\mathrm{W/m^2},\end{aligned} \tag{24}$$

close to the standard value of $4\,\mathrm{W/m^2}$.[39] The magnitude of CO_2 forcing is thus set by the gross characteristics of CO_2 spectroscopy (as embodied in l), as well as the difference in surface and stratospheric temperatures.

The formalism developed here also yields insight into the logarithmic scaling of CO_2 forcing, evident in the $\ln(q_{\mathrm{f}}/q_{\mathrm{i}})$

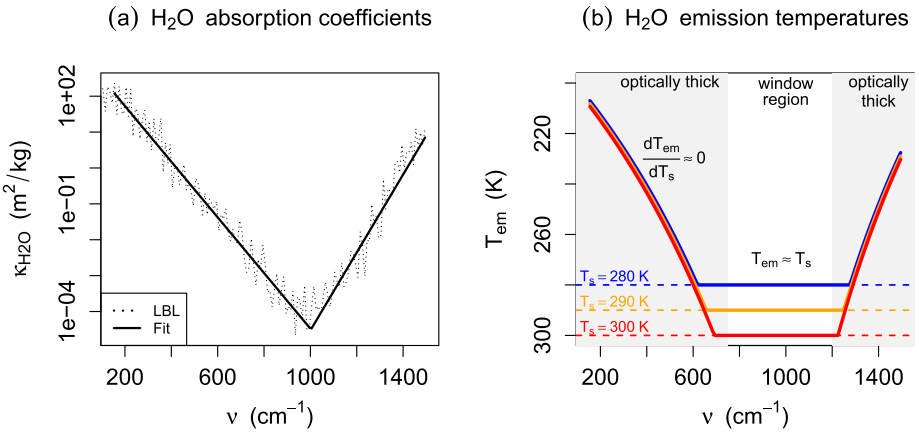

Fig. 5. (a) H_2O absorption coefficients from a line-by-line (LBL) benchmark calculation[88] at $(p_{\mathrm{ref}}, T_{\mathrm{ref}}) = (500\,\mathrm{hPa}, 260\,\mathrm{K})$, along with an exponential fit of the form (25) with $l_1 = 56\,\mathrm{cm}^{-1}$, $l_2 = 40\,\mathrm{cm}^{-1}$, $\kappa_1 = 130\,\mathrm{m}^2/\mathrm{kg}$, and $\kappa_2 = 8\,\mathrm{m}^2/\mathrm{kg}$. These absorption coefficients have been simplified by neglecting continuum absorption. (b) Graph of emission temperatures T_{em} diagnosed from Eq. (28) for $T_s = (280, 290, 300)$ K, which are insensitive to T_s except in the optically thin infrared 'window' at $750 - 1200\,\mathrm{cm}^{-1}$.

factor in Eqs. (22) and (23). Unwinding the mathematics leading to Eq. (22), one finds that the $\ln(q_f/q_i)$ factor stems from the exponential spectroscopy $\kappa_{CO_2}(\nu)$ in Eq. (19). The fact that $\kappa_{CO_2}(\nu)$ appears multiplied by q in all the relevant physical quantities [e.g., Eqs. (20) and (21)] means that a multiplicative change in q is equivalent to an additive change in ν (cf. Appendix B). Thus, multiplicative changes in q always change the width of the p_{em} triangles in Fig. 4(b) by the same $\Delta\nu$, and the forcing is proportional to this width.

V. THE WATER VAPOR FEEDBACK

Now that we have a handle on CO_2 forcing, we turn towards a better estimate of the feedback parameter λ. For λ, H_2O is the dominant GHG, as its absorption spectrum spans the entirety of the thermal infrared, as shown in Fig. 5(a) (compare the wavenumber range in Fig. 5 to that of Fig. 4; in analyzing λ we neglect the effects of CO_2 for simplicity). Similar to CO_2, the H_2O reference mass absorption coefficients $\kappa_{H_2O}(\nu)$ can be parameterized in terms of exponentials, this time with two exponentials peaked at $\nu_1 = 150\,\mathrm{cm}^{-1}$ and $\nu_2 = 1500\,\mathrm{cm}^{-1}$, as

$$\kappa_{H_2O}(\nu) = \max\left[\kappa_1 \exp\left(-\frac{|\nu-\nu_1|}{l_1}\right), \kappa_2 \exp\left(-\frac{|\nu-\nu_2|}{l_2}\right)\right]. \tag{25}$$

Note the absorption minimum at roughly $1000\,\mathrm{cm}^{-1}$, which will play an important role in what follows.[40]

Next we evaluate the optical depth integral Eq. (17). Here, ρ_{GHG} is now the water vapor density ρ_v, which we write as

$$\rho_v = \frac{p_v}{R_v T} = \frac{\mathrm{RH} p_v^*(T)}{R_v T}, \tag{26}$$

where the first equality is the ideal gas law (A2) for water vapor and the second is just a definition of the relative humidity RH, which we take to have a fixed value of 0.75.[41] Here, p_v is the partial pressure of water vapor, $R_v = 287\,\mathrm{J/(kg \cdot K)}$ is the specific gas constant for water vapor, and

$$p_v^*(T) = p_v^{\mathrm{ref}} \exp\left(-\frac{L}{R_v T}\right) \tag{27}$$

is the Clausius–Clapeyron relation for the saturation partial pressure of water vapor, with reference pressure $p_v^{\mathrm{ref}} = 2.5 \times 10^{11}$ Pa and L the latent heat of vaporization (equal to 2.5×10^6 J/kg). The Clausius–Clapeyron expression is fundamental to our RCE picture of the atmosphere, as it determines how much the water vapor content of a parcel decreases (and, hence, how much condensation is produced) per degree of cooling.

Inserting these expressions into Eq. (17) and changing the dummy integration variable from z' to T' (where the lower limit on T' is taken to be the tropopause and, thus, equals to $T_{\mathrm{strat}} = 210$ K) yield the H_2O optical depth,

$$\begin{aligned}\tau_{H_2O}(\nu, T) &= \kappa_{H_2O}(\nu) \int_{T_{\mathrm{strat}}}^{T} \frac{\mathrm{RH} p_v^{\mathrm{ref}}}{R_v T'} \frac{p(T')}{p_{\mathrm{ref}}} \exp\left(-\frac{L}{R_v T'}\right) \frac{dT'}{\Gamma} \\ &\approx \frac{p}{p_{\mathrm{ref}}} \kappa_{H_2O}(\nu) M_v^{\mathrm{ref}} \exp\left(-\frac{L}{R_v T}\right),\end{aligned} \tag{28}$$

where $T_{\mathrm{av}} \equiv (T_s + T_{\mathrm{tp}})/2$, $M_v^{\mathrm{ref}} \equiv \mathrm{RH} p_v^{\mathrm{ref}} T_{\mathrm{av}}/\Gamma L$ is a reference value for column water vapor mass ($\mathrm{kg/m^2}$), and several approximations were made to make the integral tractable.[42] Note that $M_v^{\mathrm{ref}} \exp(-L/R_v T)$ is the column mass of water vapor above the isotherm with temperature T, so Eq. (28) is just the pressure-weighted GHG mass above T times the cross-sectional area per unit mass, consistent with the interpretation in Eq. (17). Water vapor emission temperatures T_{em} can now be diagnosed by setting $\tau_{H_2O} = 1$ and inverting Eq. (28) either numerically or analytically;[43] where $\tau_{H_2O}(\nu, T_s) < 1$, in the aforementioned optically thin region centered around $1000\,\mathrm{cm}^{-1}$ (known as the infrared "window"), the emission level lies below the surface so we set $T_{\mathrm{em}} = T_s$. The results for $T_s = (280, 290, 300)$ K are plotted in Fig. 5(b).

A conspicuous feature of Fig. 5(b) is that T_{em} in the optically thick regions seems to be almost entirely insensitive to T_s, i.e., $dT_{\mathrm{em}}/dT_s \approx 0$. This can be deduced from Eq. (28), where vertical variations in τ_{H_2O} at a given ν are dominated by the temperature-dependent exponential, with the pressure-broadening factor playing only a secondary role. Thus, to a good approximation, τ_{H_2O} is a function of temperature alone, and $\tau_{H_2O}(\nu) = 1$ will occur at approximately the same T_{em} *regardless of* T_s (assuming fixed RH).

We formalize this fact, first formulated by Simpson[44] in 1928, as "Simpson's law":

Simpson's law: At fixed RH, and for optically thick wavenumbers ν dominated by H_2O absorption, emission temperatures are insensitive to surface temperature, i.e.,

$$\left.\frac{dT_{\mathrm{em}}(\nu)}{dT_{\mathrm{s}}}\right|_{\mathrm{RH}} \approx 0 \quad (\nu \text{ optically thick}).$$

This result is of course only approximate, as the pressure broadening factor (which includes a mild T_s-dependence via Eq. (10b)) and other effects cause slight deviations,[45] but we, nonetheless, refer to it as a "law" as it plays a fundamental role in governing the strength of the water vapor feedback, as follows. If $T_{\mathrm{em}}(\nu)$ and, hence, OLR_ν (by Eq. (16)) are independent of T_s for optically thick ν, and if we consider the atmosphere perfectly transparent for the optically thin ν in the window region so that OLR_ν is given by surface emission $\pi B(\nu, T_s)$ for those wavenumbers, then the spectrally resolved feedback parameter λ_ν (satisfying $\lambda = \int \lambda_\nu d\nu$) is given by

$$\lambda_\nu \equiv -\frac{d\mathrm{OLR}_\nu}{dT_s} \approx \begin{cases} 0 & (\nu \text{ optically thick}), \\ -\pi \dfrac{\partial B(\nu, T_s)}{\partial T_s} & (\text{window region}). \end{cases}$$

In other words, the feedback is zero in the optically thick regions due to Simpson's law, and in the window region is just given by the surface blackbody response. Given this, it is now straightforward to spectrally integrate λ_ν and evaluate at $T_s = 288$ K to obtain λ; all that is required is an estimate of the limits of the window region. This is typically[46] taken to be $800 < \nu < 1200\,\mathrm{cm}^{-1}$, although these limits are not precisely defined. For the sake of obtaining round numbers, we take the lower limit to be $750\,\mathrm{cm}^{-1}$, which then yields our RCE estimate of λ,[47]

$$\lambda_{\mathrm{RCE}} = -\int_{750\,\mathrm{cm}^{-1}}^{1200\,\mathrm{cm}^{-1}} \pi \frac{\partial B(\nu, T_s)}{\partial T_s}\, d\nu \approx -2\,\mathrm{W/m^2/K}, \tag{29}$$

where the integral is computed numerically. This value of λ, which was obtained here in an RCE context but in the literature is known as the "longwave clear-sky feedback" as it ignores cloud feedbacks and shortwave feedbacks, is rather universal and occurs ubiquitously throughout observational and modeling studies.[48] Furthermore, λ_{RCE} embodies the water vapor feedback discovered by MW67; by holding RH rather than specific humidity fixed, Simpson's law becomes applicable and tells us that a *significant portion of the longwave spectrum does not contribute to* λ because $T_{\mathrm{em}}(\nu)$ is fixed (Fig. 5(b)). This significantly reduces λ from the naive blackbody estimate (15) by a factor of about 2, consistent with MW67's early finding that the water vapor feedback doubles climate sensitivity.

Indeed, a feedback parameter of $\lambda_{\mathrm{RCE}} = -2\,\mathrm{W/m^2/K}$, combined with $\mathcal{F}_{2\times} = 4\,\mathrm{W/m^2}$, yields an estimated equilibrium climate sensitivity of

$$\mathrm{ECS}_{\mathrm{RCE}} = -\frac{\mathcal{F}_{2\times}}{\lambda_{\mathrm{RCE}}} \approx 2\,\mathrm{K}. \tag{30}$$

This estimate is close to those obtained by MW67 (2.3–2.9 K) though somewhat smaller than the consensus value of 3 K. Given the evidence that the neglected cloud and shortwave feedbacks are likely positive, however (see Sec. VI), it is unsurprising that $\mathrm{ECS}_{\mathrm{RCE}}$ is biased low, and it is perhaps best regarded as a lower bound on ECS. Indeed, 2 °C is the lower bound of the very likely range of 2–5 °C found in the recent sixth assessment report of the IPCC.[49]

VI. BEYOND RCE: ADDITIONAL FEEDBACKS

In this less detailed section, we sketch the phenomena unaccounted for in the RCE framework, discuss their impacts on λ and ECS as assessed with numerical simulations and observations, and discuss prospects for principled estimates similar in spirit to those presented above.

A. Clouds

A major omission from the framework developed so far is clouds. Clouds exert enormous leverage over the climate system by absorbing and emitting longwave radiation essentially as blackbodies, and also by reflecting shortwave radiation (roughly half of Earth's albedo is due to clouds[50]). In the longwave, certain aspects of the radiative effects of clouds can be described with a relatively simple formalism, as follows.[51]

The longwave effects of clouds stem primarily from the high clouds arising from thunderstorms and mid-latitude winter storms; consistent with their height these clouds are very cold with a typical cloud-top temperature $T_{\mathrm{cld}} = 220$ K (Fig. 2). Their Planck emission is, thus, much reduced relative to the clear-sky OLR one would see in their absence. If these high clouds cover a fraction f of the Earth's surface ($f \approx 0.18$ in the present-day global mean[52]), then one can write the "all-sky" (i.e., actual) OLR as

$$\mathrm{OLR}_{\mathrm{all}} = (1-f)\mathrm{OLR}_{\mathrm{clr}} + f\sigma {T_{\mathrm{cld}}}^4. \tag{31}$$

In other words, high clouds mask a fraction f of $\mathrm{OLR}_{\mathrm{clr}}$, replacing it with cloud-top emission $\sigma {T_{\mathrm{cld}}}^4$.

To differentiate Eq. (31) and obtain the all-sky longwave feedback λ_{all}, one needs to know how f and T_{cld} respond to warming. Fortunately, the latter question is answered quite simply by the so-called *fixed anvil temperature* hypothesis,[53] which is related to Simpson's law and says that high clouds rise with global warming so as to keep T_{cld} fixed, i.e.,

$$\frac{dT_{\mathrm{cld}}}{dT_{\mathrm{s}}} \approx 0. \tag{32}$$

Differentiating Eq. (31), thus, yields

$$\lambda_{\mathrm{all}} = (1-f)\lambda_{\mathrm{clr}} + \frac{df}{dT_{\mathrm{s}}}(\mathrm{OLR}_{\mathrm{clr}} - \sigma {T_{\mathrm{cld}}}^4). \tag{33}$$

As for df/dT_s, f is generally expected to decrease with warming (a feedback known as the "iris effect"),[54] but the magnitude of this decrease is uncertain and there is as yet insufficient theory to estimate it from first principles. The terms in Eq. (33) related to f and df/dT_s, thus, tend to compensate, and the value

of λ_{all} ends up not far from $\lambda_{\text{clr}} \approx -2\,\text{W/m}^2/\text{K}$ but with larger error bars.[55]

On the shortwave side, there are highly reflective subtropical marine low clouds whose areal coverage is thought to decrease with global warming, yielding an increase in absorbed sunlight with warming and, thus, a positive contribution to the total feedback parameter of $\lambda_{\text{cld}}^{\text{SW}} \sim 0.2\,\text{W/m}^2/\text{K}$.[56] This decrease in coverage is often understood via changes in environmental variables known as "cloud-controlling factors" such as the local sea surface temperature and relative humidity; sophisticated analyses of these dependencies allow us to quantify the associated feedback.[57] Meanwhile, these clouds have also been described by simplified "mixed-layer models."[58] However, these dots so far remain unconnected, and a first principles estimate of the tropical marine low cloud feedback also remains unformulated.

B. Shortwave feedbacks

In addition to changes in sunlight reflected by clouds, there are other significant shortwave feedbacks (i.e., changes in absorbed solar radiation S with warming) left unaccounted for in the RCE framework. Perhaps the largest of these is the *surface-albedo* feedback, due primarily to decreasing snow and ice cover with warming, which manifests as changes in albedo α [cf. Eq. (1)]. This yields a positive feedback $\lambda_{\text{albedo}} \sim 0.3$–$0.4\,\text{W/m}^2/\text{K}$.[59] While highly idealized models of the ice-albedo feedback have existed for decades,[60] and comprehensive modeling studies reveal a close connection between this feedback and the seasonal cycle,[61] again this gap has not been bridged and a chalkboard estimate of the surface-albedo feedback has yet to be formulated.

Another shortwave feedback, which receives less attention but is not insignificant, is that due to shortwave absorption by water vapor. Though often neglected in introductory treatments such as that of Sec. II, it turns out that water vapor absorbs a rather significant amount of near-infrared sunlight—around $80\,\text{W/m}^2$.[62] Since the mass of water vapor in the atmosphere increases with warming [at a rate roughly dictated by the Clausius–Clapeyron relation (27)],[63] water vapor shortwave absorption also increases, reducing the amount of (near-infrared) sunlight reflected out to space and, thus, increasing S. The end result is a positive shortwave water vapor feedback $\lambda_{\text{wv}}^{\text{SW}} \sim 0.25\,\text{W/m}^2/\text{K}$.[64] A principled estimate of $\lambda_{\text{wv}}^{\text{SW}}$ may be fairly easy to obtain, leveraging the fact that water vapor shortwave absorption should be a fixed function of temperature (i.e., it obeys its own version of Simpson's law), in analogy to water vapor longwave emission.[65]

C. The total feedback

Putting the RCE (or longwave clear-sky) estimate (29) together with the cloud and shortwave feedbacks outlined above yields an estimate for the total feedback parameter

$$\lambda_{\text{tot}} \approx \underbrace{\lambda_{\text{RCE}}}_{-2} + \underbrace{\lambda_{\text{cld}}^{\text{SW}}}_{0.2} + \underbrace{\lambda_{\text{albedo}}}_{0.3-0.4} + \underbrace{\lambda_{\text{wv}}^{\text{SW}}}_{0.25} \approx -1.2\ \text{W/m}^2/\text{K}. \tag{34}$$

This is close to the value of $\lambda = -1.3\,\text{W/m}^2/\text{K}$ assessed by Sherwood *et al.*[66] from multiple lines of evidence, which indeed yields the consensus ECS value of $-\mathcal{F}_{2\times}/\lambda = (4\,\text{W/m}^2)/(1.3\,\text{W/m}^2/\text{K}) \approx 3\,\text{K}$. This more realistic value of λ will be a key ingredient in estimating other measures of climate sensitivity, which we take up in Sec. VII.

VII. BEYOND ECS: OTHER MEASURES OF CLIMATE SENSITIVITY

In this final section, we look beyond ECS to other measures of climate sensitivity. We will find that ECS is a quite idealized notion, and that other measures of climate sensitivity are more relevant for present-day warming and for understanding and defining emissions targets. However, we will also see that ECS, as well as its key ingredients $\mathcal{F}$ and λ, naturally appear in these other measures. Thus, the basic understanding of ECS developed here is necessary for understanding these other measures.

A. The deep ocean and timescales of global warming

The equilibrium climate sensitivity is exactly that: An equilibrium quantity. However, how *long* does it take the climate system to equilibrate with a given CO_2 concentration, and what does this evolution look like? To address this, we need a time-dependent model of the Earth's surface temperature T_s. We proceed by neglecting the dynamics of the land surface (since the Earth is roughly 2/3 ocean covered) and invoking the popular *two-layer* or *two-box* model for the ocean.[67] This model consists of a shallow mixed layer with depth $h_{\text{ml}} \approx 50\,\text{m}$ and temperature anomaly T'_{ml} equal to ΔT_s, sitting atop a much larger deep ocean with global average depth $h_d \approx 2500\,\text{m}$ and temperature anomaly T'_d. The model is pictured in Fig. 6.

An important characteristic of this model is that if the mixed layer is warmed by a forcing $\mathcal{F}$, it both radiates extra energy to space at a rate of $|\lambda|T'_{\text{ml}}$ and also *exports energy to the deep ocean*, which we parameterize in linearized form as $\gamma(T'_{\text{ml}} - T'_d)$ (units of W/m^2). Here, γ is the "deep ocean heat uptake efficiency," estimated from models at roughly $0.7\,\text{W/m}^2/\text{K}$.[68] Setting ρ_w and C_w as the densities and specific heat capacities of water, the corresponding equations are

$$\rho_w C_w h_{\text{ml}} \frac{dT'_{\text{ml}}}{dt} = \mathcal{F} - |\lambda|T'_{\text{ml}} - \gamma(T'_{\text{ml}} - T'_d), \tag{35a}$$

$$\rho_w C_w h_d \frac{dT'_d}{dt} = \gamma(T'_{\text{ml}} - T'_d). \tag{35b}$$

Because the deep ocean has a much larger depth and, hence, heat capacity than the mixed layer ($h_d \gg h_{\text{ml}}$), we expect T'_{ml} to respond to $\mathcal{F}$ much faster than T'_d does. Indeed, assuming $T'_d = 0$ in Eq. (35a) yields a linear,

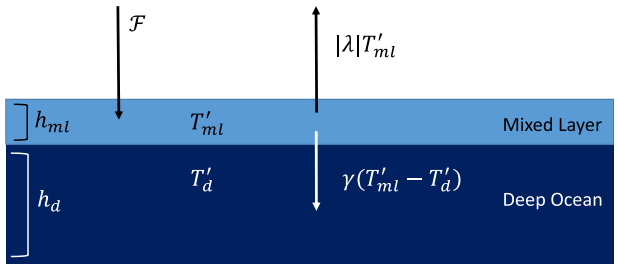

Fig. 6. Two-box model for the ocean. See the text for discussion.

constant coefficient ordinary differential equation with characteristic timescale,

$$\tau_{\mathrm{ml}} = \frac{\rho_w h_{\mathrm{ml}} C_w}{\gamma + |\lambda|} \approx 3\,\mathrm{years}. \tag{36}$$

If we now consider timescales longer than τ_{ml}, we may set $dT'_{\mathrm{ml}}/dt = 0$ in Eq. (35a), solve for T'_{ml}, plug the result into Eq. (35b), and solve for the characteristic deep ocean timescale τ_d. This makes a nice exercise with result

$$\tau_d = \rho_w h_d C_w \frac{\gamma + |\lambda|}{\gamma |\lambda|} \approx 700\,\mathrm{years}. \tag{37}$$

Thus, the vast difference in total heat capacity between the mixed layer and deep ocean indeed leads to two timescales for global warming: A "fast" timescale of about $\tau_{\mathrm{ml}} \approx 3$ years during which the mixed layer equilibrates (really a "quasi-equilibrium," since this equilibrium state will change as the deep ocean slowly responds), and a "slow" timescale of $\tau_d \approx 700$ years during which the deep ocean equilibrates (a true equilibrium). On intermediate timescales in between τ_{ml} and τ_d in which the mixed layer is in quasi-equilibrium, we can assume both $dT'_{\mathrm{ml}}/dt = 0$ and $T'_d \approx 0$, which from Eq. (35a) yields

$$T'_{\mathrm{ml}} \approx \frac{\mathcal{F}}{\gamma + |\lambda|} \quad (\text{quasi-equilibrium}). \tag{38}$$

This gives the transient warming which occurs before the deep ocean has responded. Indeed, if we specialize to the case of a CO_2 doubling, the temperature in Eq. (38) becomes a standard sensitivity metric known as the "transient climate response," or TCR,[69]

$$\mathrm{TCR} = \frac{\mathcal{F}_{2\times}}{\gamma + |\lambda|} \approx 2\,\mathrm{K}. \tag{39}$$

This estimate is quite close to the value of 1.8 K found in the recent sixth assessment report of the IPCC.[70] Comparing Eq. (39) with Eq. (13) shows that ECS > TCR: on the intermediate timescales during which $T'_{\mathrm{ml}} = \mathrm{TCR}$, the mixed layer is both radiating heat to space *and* exporting heat to the deep ocean (Fig. 6) and can, thus, come to (quasi-)equilibrium at a lower temperature. This is of course not a true equilibrium state, and one can interpret the ratio TCR/ECS as a measure of the ocean's thermal disequilibrium; this measure will prove useful in Sec. VII B.

A key assumption in Eqs. (38) and (39) is that $T'_d \approx 0$ on intermediate timescales. This approximation turns out to be a reasonable description of the present day, and the quasi-equilibrium formula (38) (which is just a scaling of TCR) can be used to credibly model historical as well as near-term global warming.[71] In these ways, TCR is a more relevant metric for present day climate change than ECS, which instead assumes that both the mixed layer *and* deep ocean have reached a mutual equilibrium, which from Eq. (37) would take many hundreds of years.[72]

Note that the two-box model, while popular, is by no means canonical. Some recent work instead employs three-box models, and the older literature often employed diffusive models.[73] Two-box, three-box, and diffusive models were all employed by the IPCC as emulators of more comprehensive models.[74] All these approaches, however, require empirically determined parameters for heat transfer coefficients and diffusivities, analogous to our heat uptake efficiency γ, and principled estimates for these quantities are still lacking.[75]

B. The carbon cycle and measures of carbon-climate sensitivity

In addition to only describing very long-term warming, another limitation of ECS is that it assumes that the perturbed CO_2 concentration q is *constant* while the Earth system equilibrates. If we stop burning fossil fuels, however, q will not remain constant; the real Earth has an active carbon cycle in the land and ocean, both of which absorb significant amounts of anthropogenic CO_2, which would cause q to decrease over time. Full consideration of these dynamics leads to two additional measures of climate sensitivity which are fundamental for both climate change science as well as policy: the *transient climate response to cumulative emissions* (TCRE) and the *zero emissions commitment* (ZEC).

TCRE is defined to be the warming at a given time divided by the *cumulative* emissions released prior to that time, in Kelvins per gigaton of carbon (K/GtC). TCRE is found to have a characteristic value of $\sim 2\,\mathrm{K}/1000\,\mathrm{GtC}$, which in simulations turns out to be fairly invariant over time as well as insensitive to emissions scenario.[76] The robustness of TCRE tells us that any identified temperature target (e.g., $\Delta T_s = 1.5$ or $2\,^\circ\mathrm{C}$) automatically reduces to a cumulative emissions target (e.g., 750 or 1000 GtC), which can only be met if we *cease* emissions prior to reaching the target. This leads directly to the notion of net zero emissions.[77]

It is possible to use the TCR of Sec. VII A, as well as the logarithmic scaling of CO_2 forcing, to make a back-of-the-envelope estimate of TCRE as follows. Let C_{emit} be our cumulative carbon emissions since the preindustrial era (GtC), C_{pre} the preindustrial mass of CO_2 in the atmosphere (GtC), and α be the fraction of C_{emit} still residing in the atmosphere (the "airborne fraction"), so that the total mass of CO_2 in the atmosphere is $C_{\mathrm{pre}} + \alpha C_{\mathrm{emit}}$. Recalling that in the quasi-equilibrium approximation, surface warming ΔT_s can be obtained by scaling the TCR by $\mathcal{F}/\mathcal{F}_{2\times}$ [cf. Eqs. (38) and (39)], we then have

$$\begin{aligned}
\mathrm{TCRE} &\equiv \frac{\Delta T_s}{C_{\mathrm{emit}}} \\
&= \frac{\mathcal{F}}{\mathcal{F}_{2\times}} \frac{\mathrm{TCR}}{C_{\mathrm{emit}}} \quad \text{by (38) and (39)} \\
&= \frac{\ln\left(\dfrac{C_{\mathrm{pre}} + \alpha C_{\mathrm{emit}}}{C_{\mathrm{pre}}}\right)}{\ln 2} \frac{\mathrm{TCR}}{C_{\mathrm{emit}}} \quad \text{by (23)} \\
&\approx \frac{\alpha}{\ln 2} \frac{\mathrm{TCR}}{C_{\mathrm{pre}}} \quad \text{using } \ln(1+x) \approx x\,.
\end{aligned} \tag{40}$$

In the last equality, C_{emit} drops out of this expression, giving some insight into why simulations find TCRE to be roughly invariant over time.[78] Furthermore, evaluating Eq. (40) for $C_{\mathrm{pre}} = 590\,\mathrm{GtC}$ and the present day airborne fraction of $\alpha = 0.4$ indeed yields roughly 2 K/GtC, consistent with simulations.[79] However, here we are simply using the observed value of α; we do not yet have ways to make principled estimates of α from basic carbon cycle dynamics, and thus to

understand how and why α does or does not vary across time and emissions scenarios.

The zero emissions commitment (ZEC), on the other hand, is complementary to TCRE and is defined to be the amount of residual warming occurring *after emissions cease*. Simulations[80] tend to show that ZEC is small relative to ΔT_s, which is a requirement for net zero emissions goals to meaningfully limit ΔT_s. Similar to the estimate for TCRE, we may scale TCR and also ECS to estimate ZEC, following an argument due to Tarshish.[81] Let T_{ze} and α_{ze} be the temperature and airborne fraction of cumulative emissions when emissions cease, and T_f and α_f be the temperature and airborne fraction at final equilibrium, respectively. Normalizing $\text{ZEC} \equiv T_f - T_{ze}$ by T_{ze}, we have

$$\begin{aligned}\frac{\text{ZEC}}{T_{ze}} &= \frac{T_f}{T_{ze}} - 1 \\ &= \frac{\ln\left(\frac{C_{pre} + \alpha_f C_{emit}}{C_{pre}}\right)\text{ECS}}{\ln\left(\frac{C_{pre} + \alpha_{ze} C_{emit}}{C_{pre}}\right)\text{TCR}} - 1 \quad \text{by (13), (23), (39)} \\ &\approx \frac{\alpha_f/\alpha_{ze}}{\text{TCR}/\text{ECS}} - 1\,. \end{aligned} \tag{41}$$

This tells us that the sign and magnitude of ZEC is determined by a competition between the chemical disequilibrium α_f/α_{ze} and thermal disequilibrium TCR/ECS when emissions cease. If the chemical disequilibrium is more pronounced than the thermal disequilibrium, i.e., if $\alpha_f/\alpha_{ze} < \text{TCR}/\text{ECS}$, then the decline in CO_2 forcing due to equilibrium carbon uptake will dominate over the reduction in the deep ocean heat sink, yielding $\text{ZEC} < 0$, and vice-versa if $\alpha_f/\alpha_{ze} < \text{TCR}/\text{ECS}$. Noting that $\alpha_f \approx 0.2$ is a characteristic value, which may be obtained from principles of carbonate chemistry,[82] the previously cited values $\alpha_{ze} = 0.4$, TCR $= 1.8$ K, and ECS $= 3$ K then give $\text{ZEC}/T_{ze} \approx -0.17$, which is indeed small (and, perhaps surprisingly, negative).

While Eq. (41) appears to explain why ZEC is small, it is only a proximal explanation. The heat uptake efficiency γ, which entered into our estimate Eq. (39) of TCR, as well as the present day airborne fraction $\alpha \approx 0.4$, were evaluated via simulations or observations rather than theoretically, so we do not yet have fully principled estimates for TCRE or ZEC. Such estimates would necessarily draw upon physics from across the Earth system, including the dynamics of ocean heat uptake, ocean carbon uptake, CO_2 fertilization of the biosphere, and more. A chalkboard explanation of these quantities, thus, poses a grand challenge to climate science; the simple models presented here are simply a first step towards that goal.

ACKNOWLEDGMENTS

This article grew out of notes prepared for lectures hosted by the Princeton Geosciences department, Princeton Environmental Institute (PEI), and the Princeton Program in Atmosphere and Ocean Sciences in January 2018.[83] The author would like to thank Robert Socolow and Mike Celia of PEI for the encouragement to develop and deliver these lectures; Isaac Held, Stephan Fueglistaler, and Yi Ming for continued support and constructive feedback; Nathaniel Tarshish, Brett McKim, and Sam Schulz for detailed comments; and Tapio Schneider and Brett McKim for encouragement to publish.

AUTHOR DECLARATIONS

Conflict of Interest

No conflict of interest to disclose.

APPENDIX A: ADIABATIC TEMPERATURE PROFILES

We here derive expression (5) for the dry adiabatic lapse rate. For a textbook treatment of this topic, as well as extension to include the effects of moisture, see, e.g., the textbook by Wallace and Hobbs[84] or the excellent lecture notes of Romps.[85]

Consider a rising convective parcel that conserves its mass and rises rapidly such that heat exchange with the environment is negligible. This process is governed by the first law of thermodynamics,

$$dQ = dU + p\,dV, \tag{A1}$$

where dQ is the heat gained by the system, U is its internal energy, p is its pressure, and V is its volume. For an ideal gas, we have $U = \rho V C_v T$ as well as the ideal gas law, written in the form typical of atmospheric science,

$$p = \rho R_d T, \tag{A2}$$

where ρ is the parcel density in kg/m^3, $R_d = 287\,\text{J/kg/K}$ is the specific gas constant for dry air (obtained by dividing the universal gas constant by the molar mass of air), and $C_v = (5/2)R_d$ is the specific heat capacity at constant volume. Assuming an adiabatic process ($dQ = 0$), we rearrange Eq. (A1) into

$$0 = \rho C_p\,dT - dp,$$

where the specific heat at constant pressure $C_p = C_v + R_d \approx 1000\,\text{J/kg/K}$. Further assuming hydrostatic balance,[86] which says that the weight of a layer of air is balanced by the vertical pressure gradient across it,

$$\frac{dp}{dz} = -\rho g, \tag{A3}$$

and rearranging then yields Eq. (5)

$$\Gamma_d \equiv -\frac{dT}{dz} = \frac{g}{C_p}.$$

Now consider an arbitrary but constant lapse rate Γ. Then, we have

$$\frac{dT}{dp} = \frac{dT}{dz}\frac{dz}{dp} = \frac{\Gamma}{\rho g} = \frac{\Gamma R_d T}{pg}, \tag{A4}$$

where Eq. (A3) was used in the second equality and Eq. (A2) in the third. This relation between T and p can be integrated from an arbitrary pressure p to surface pressure p_s to obtain Eq. (10b).

APPENDIX B: ANALYTIC DERIVATION OF FORMULA FOR CO_2 FORCING

The forcing $\mathcal{F}$ is usually obtained by numerical integration in ν across the CO_2 band shown in Fig. 4. Here, we will instead pursue an analytical integration over ν, following the thesis of Seeley.[87] We will take advantage of the symmetry evident in Fig. 4 and simply double the integral for $\nu > \nu_0$. We will also take advantage of the key fact that q and $\kappa_{CO_2}(\nu)$ appear in Eq. (20) as a product; this, along with the exponential spectroscopy Eq. (19) and the fact that T_{em} and p_{em} are related by Eq. (10b), means that

$$\frac{dT_{em}}{d\ln q} = \frac{dT_{em}}{d\ln \kappa_{CO_2}} = -l\frac{dT_{em}}{d\nu}. \tag{B1}$$

This equation encapsulates the fact, mentioned towards the end of Sec. IV, that a multiplicative change in q is equivalent to that of a uniform translation in ν. Putting these ingredients together, the forcing Eq. (11) can now be evaluated as an integral over ν from band center ν_0 to the upper limit $\nu_+ \approx 750\,\mathrm{cm}^{-1}$, where we ignore spectral variations in the Planck density. This yields

$$\begin{aligned}
\mathcal{F} &= -(\Delta \ln q)\frac{d\mathrm{OLR}}{d\ln q},\\
&= -2\ln(q_f/q_i)\int_{\nu_0}^{\nu_+}\frac{d\mathrm{OLR}_\nu}{d\ln q}d\nu,\\
&= -2\ln(q_f/q_i)\int_{\nu_0}^{\nu_+}\pi\frac{\partial B}{\partial T}\frac{dT_{em}}{d\ln q}d\nu \quad \text{by Eq. (16)},\\
&= 2l\ln(q_f/q_i)\int_{\nu_0}^{\nu_+}\pi\frac{\partial B}{\partial T}\frac{dT_{em}}{d\nu}d\nu \quad \text{by Eq. (B1)},\\
&= 2l\ln\left(\frac{q_f}{q_i}\right)[\,\pi B(\nu_0,T_s) - \pi B(\nu_0,T_{strat})\,],
\end{aligned}$$

where in the last line we invoked the fundamental theorem of calculus, noting also that $T_{em}(\nu_+) = T_s$ and $T_{em}(\nu_0) = T_{strat}$.

[1] Arrhenius (1896).
[2] Sherwood *et al.* (2020); Forster *et al.* (2021).
[3] The report of Charney *et al.* (1979) was the first such model intercomparison report. Meehl *et al.* (2020) reviewed ECS over the many generation of IPCC reports. The latest IPCC assessment of ECS is given in Chapter 7 of the sixth assessment report from working group I, Forster *et al.* (2021), Sec. 7.5; see also the comprehensive ECS review in Sherwood *et al.* (2020).
[4] Manabe and Wetherald (1967).
[5] Jeevanjee *et al.* (2022).
[6] Wilson and Gea-Banacloche (2012); Jeevanjee *et al.* (2021b); Romps *et al.* (2022).
[7] Koll and Cronin (2018); Jeevanjee (2018); Jeevanjee *et al.* (2021a).
[8] For a similar but not explicitly pedagogical approach, see also Stevens and Kluft (2023).
[9] Hartmann (2015).
[10] Pierrehumbert (2011).
[11] He *et al.* (2022) is an example of this, in which the formalism for CO_2 forcing developed here is applied to understand the spread in that quantity amongst comprehensive climate models.
[12] For a related point of view, see Emanuel (2020).
[13] Trenberth and Fasullo (2009); Stephens *et al.* (2015).
[14] See Sec. VI B and Note 65 for more on this approximation.
[15] For example, Petty (2006); Randall (2012); Vallis (2012); Coakley Jr., and Yang (2014); Hartmann (2015); Tziperman (2022).
[16] Thermodynamically speaking, this is a steady-state, not an equilibrium, as the net fluxes of e.g., solar radiation, thermal radiation, water vapor at the Earth's surface, etc., are nonzero. Accordingly, the Earth does not come into thermal equilibrium with either the Sun or outer space but tends towards a temperature in between them. Nonetheless, the use of the term "equilibrium" to describe a steady-state in climate is ubiquitous, so we adopt this terminology here.
[17] It is a nice exercise to derive this height analytically, as follows: Assume an isothermal atmosphere with $T = T_{em}$, which from Eqs. (A3) and (A2) yields the exponential dependence

$$p = (1\,\mathrm{atm})\exp(-z/H), \tag{B2}$$

where $H \equiv R_d T_{em}/g \approx 7.5\,\mathrm{km}$ is the atmospheric "scale height." Setting $p_a = 0.5$ atm then yields $z_a = H\ln 2 \approx 5\,\mathrm{km}$. Note also that in this isothermal approximation, and by the ideal gas law (A2), $\rho \sim p/T$ also declines exponentially with height.
[18] Hansen *et al.* (1981).
[19] Payne *et al.* (2015).
[20] Stratospheric temperatures are sometimes thought to be governed by the so-called "skin temperature," which arises by considering an optically thin layer of atmosphere sitting atop the troposphere; a standard argument yields a skin temperature of $T_{em}/\sqrt[4]{2} = 214$ K (Pierrehumbert, 2011; Hartmann, 2015). This argument ignores the strong dependence of tropopause and stratospheric temperatures on atmospheric composition, however (e.g., Manabe and Strickler, 1964). Recent work instead postulates that T_{strat} is governed by the physics of H_2O radiative transfer (Seeley *et al.*, 2019; Jeevanjee and Fueglistaler, 2020b), but more work on this topic is needed.
[21] At least to first approximation. See discussion in Jeevanjee *et al.* (2022).
[22] This is the ratio of the mass of a given substance in a parcel to the total mass of the parcel. For further discussion, see Pierrehumbert (2011), p. 87.
[23] While such a perspective ignores the interactive carbon cycle dynamics of the atmosphere, land, and ocean, it is, nonetheless, a useful starting point for understanding the impacts of fossil-fuel combustion on Earth's climate. We discuss how carbon cycle dynamics modify the picture presented here in Sec. VI.
[24] There are, however, processes known as atmospheric *adjustments* which blur this distinction; see Sherwood *et al.* (2015).
[25] An important exception to this reasoning is the *stratospheric adjustment*, which is the direct response of stratospheric temperatures to a change in q resulting from the increased emission to space depicted in Fig. 4(b) (green dashed lines). This change in stratospheric temperatures occurs independently of changes in T_s, precisely because the stratosphere is not coupled to the surface in the way the troposphere is. For further discussion, see Hansen *et al.* (1997); Houghton *et al.* (1994).
[26] Another useful consequence of this definition is that "positive," amplifying feedbacks make positive contributions to λ.
[27] Charney *et al.* (1979); Myhre *et al.* (1998); Ramaswamy *et al.* (2019).
[28] We will not need the specific form of $B(\nu,T)$, but for completeness, it is given by

$$B(\nu,T) = \frac{2h\nu^3}{c^2}\frac{1}{\exp\left(\frac{h\nu}{k_bT}\right) - 1}, \tag{B3}$$

where h is Planck's constant, k_b is Boltzmann's constant, and c is the speed of light.
[29] Since CO_2 is well-mixed, its density is proportional to the air density ρ, and ρ decreases exponentially with height (cf. Note 17). For H_2O, its density is dominated by its Clausius–Clapeyron exponential dependence on temperature (Eqs. (26) and (27)), and temperature is linear in height, so H_2O density is exponential in height as well.
[30] We here assume a two-stream approximation with unit diffusion coefficient for simplicity (Pierrehumbert, 2010).
[31] This pressure scaling is due to collisional pressure broadening away from spectral line centers and is also accompanied by additional, typically less pronounced temperature scalings. See Pierrehumbert (2010).
[32] For further analysis of the emission level approximation, with analytic calculations suitable for the classroom, see Appendix B of Jeevanjee *et al.* (2021b) and Appendix B of Jeevanjee and Fueglistaler (2020a).
[33] Wilson and Gea-Banacloche (2012).
[34] Seeley (2018).
[35] Jeevanjee *et al.* (2021b).
[36] Romps *et al.* (2022).
[37] Jeevanjee *et al.* (2021b).
[38] For a pedagogical discussion of the structure of this spectrum and its computation, see Wilson and Gea-Banacloche (2012).

[39]This estimate ignores several effects, each of which generate 20%–30% corrections but which offset each other. These effects include the overlapping of CO_2 absorption by H_2O absorption, the masking of CO_2 forcing by clouds, and stratospheric adjustment. See Jeevanjee *et al.* (2021b); Huang *et al.* (2016).

[40]The H_2O absorption coefficients shown here have been simplified by neglecting so-called "continuum" absorption. Continuum absorption significantly affects absorption in the infrared window at warmer surface temperatures of 300 K and above. See Pierrehumbert (2010); Shine *et al.* (2012); Koll *et al.* (2022).

[41]This fixed relative humidity assumption, popularized by Manabe and Wetherald (1967), has been well justified by decades of subsequent simulations and observation (Jeevanjee *et al.*, 2022; Colman and Soden, 2021).

[42]In particular, we multiply the integrand by T_{av}/T', which does not deviate too far from 1 but which allows the exponential to be integrated. Since the integrand is dominated by values of the exponential evaluated near T, we also approximate $p(T') \approx p(T)$ so it can be pulled outside the integral. This expression and these approximations are discussed in more detail in Jeevanjee and Fueglistaler (2020b).

[43]Equation (28) can be inverted at $\tau = 1$ using the Lambert W function to obtain

$$T_{\text{em}}(\nu) = \frac{T^*}{W\left(\frac{T^*}{T_{\text{ref}}}\left(D\,M_v^{\text{ref}}\kappa_{H_2O}(\nu)\right)^{R_d\Gamma/g}\right)}, \quad \text{where } T^* = \frac{LR_d\Gamma}{gR_v}.$$

See also Jeevanjee and Fueglistaler (2020b).

[44]See, e.g., Simpson (1928). See also Ingram (2010); Jeevanjee *et al.* (2021a) for further discussion.

[45]These deviations can be estimated by calculating dT_{em}/dT_s implicitly from Eq. (28) and invoking Eq. (10b). This makes a nice exercise, with result

$$\frac{dT_{\text{em}}}{dT_s} = \frac{T_{\text{em}}}{T_s}\frac{1}{\frac{LR_d\Gamma}{gR_vT_{\text{em}}} - 1} \approx \frac{1}{4}. \tag{B4}$$

[46]Petty (2006).

[47]This approach has precedent in the work of Koll and Cronin (2018); Ingram (2010).

[48]Koll and Cronin (2018); Zhang *et al.* (2020); McKim *et al.* (2021); Colman and Soden (2021).

[49]Forster *et al.* (2021), Table 7.13.

[50]Stephens *et al.* (2015).

[51]See McKim et al. (2021); Stevens and Kluft (2023); McKim et al. (2023).

[52]We obtain $f = 0.18$ as an average of the AIRS and ISCCP satellite data values for global mean high cloud fraction given in Fig. 4.5 of Siebesma *et al.* (2020).

[53]Hartmann and Larson (2002); Thompson *et al.* (2017); Jeevanjee and Fueglistaler (2020b).

[54]Mauritsen and Stevens (2015); Bony *et al.* (2016).

[55]For example, Andrews *et al.* (2015); Flynn and Mauritsen (2020).

[56]Zelinka *et al.* (2016); Klein *et al.* (2017); Sherwood *et al.* (2020).

[57]Myers *et al.* (2021); Ceppi and Nowack (2021).

[58]Lilly (1968); Bretherton and Wyant (1997).

[59]Zelinka *et al.* (2020); Colman (2013).

[60]North *et al.* (1981).

[61]Hall (2004).

[62]See Trenberth and Fasullo (2009). It is an interesting exercise with the RCE model Eq. (8) to show that subtracting this from the surface energy budget and adding it to the atmospheric energy budget does not affect T_s, consistent with the interpretation that the atmosphere and surface function as a unit so repartitioning energy between them do not affect their temperatures.

[63]Held and Soden (2006).

[64]Donohoe *et al.* (2014).

[65]Jeevanjee (2018).

[66]Sherwood *et al.* (2020).

[67]Schneider and Thompson (1981); Gregory (2000); Held *et al.* (2010); Armour (2017).

[68]Geoffroy *et al.* (2013).

[69]Strictly speaking, TCR is defined via simulations in which CO_2 is increased from its preindustrial value at 1% year until the concentration has doubled, and TCR is defined as the warming at the time of doubling (around year 70). However, it has been shown that the two-box expression (39) for TCR captures the actual TCR fairly well (Held *et al.*, 2010; Geoffroy *et al.*, 2013).

[70]Forster *et al.* (2021), Sec. 7.5.5.

[71]Held *et al.* (2010); Geoffroy *et al.* (2013).

[72]Indeed, it is a simple exercise to show that imposing the full equilibrium conditions $dT'_{\text{ml}}/dt = dT'_d/dt = 0$ in Eqs. (35) for $\mathcal{F} = \mathcal{F}_{2\times}$ yields $T'_{\text{ml}} = T'_d = \mathcal{F}_{2\times}/|\lambda| = \text{ECS}$.

[73]Three-box models were employed in, e.g., Proistosescu and Huybers (2017); Cummins *et al.* (2020); Tsutsui (2020). Diffusive models were employed in, e.g., Hansen (1984); Siegenthaler and Oeschger (1984); Wigley and Schlesinger (1985).

[74]See Chapter 7 of the IPCC sixth assessment report (Forster *et al.*, 2021), and in particular, cross-chapter box 7.1. Two popular emulators employed there are MAGICC (Meinshausen *et al.*, 2011), which has a diffusive deep ocean, and FaIR (Leach *et al.*, 2021), which has a three-box ocean.

[75]Though there has been some work in this direction; see e.g., Marshall and Zanna (2014).

[76]MacDougall (2016).

[77]Allen *et al.* (2022).

[78]Additional insight can be found in the theoretical approaches of, e.g., Goodwin *et al.* (2015); MacDougall and Friedlingstein (2015); Seshadri (2017).

[79]Friedlingstein *et al.* (2020) provide values of C_{pre} and α. It is also a nice exercise to estimate C_{pre} by multiplying the mass of the atmosphere $4\pi R_E^2 p_s/g$ by the specific CO_2 concentration corresponding to the number concentration of 280 ppm. Note also that for present-day C_{emit} of roughly 700 GtC, we have $\alpha C_{\text{emit}}/C_{\text{pre}} \approx 0.45$, so the approximation $\ln(1 + \alpha C_{\text{emit}}/C_{\text{pre}}) \approx \alpha C_{\text{emit}}/C_{\text{pre}}$ used in Eq. (40) is marginally acceptable, but will fail for larger C_{emit}.

[80]MacDougall *et al.* (2020).

[81]Tarshish *et al.* (2022).

[82]Goodwin *et al.* (2007).

[83]The original notes contain additional material beyond that presented here; see Jeevanjee (2018).

[84]Wallace and Hobbs (2006).

[85]Romps (2020).

[86]There is some sleight-of-hand here, as hydrostatic balance typically applies to the pressure and density of the quiescent *environment*, rather than a rising parcel. For most applications (such as ours), this approximation is permissible, but if we take it to extremes (such as applying the dry adiabatic lapse rate Eq. (5) over large enough distances to generate negative temperatures) it can lead to nonsensical results; for further discussion see Romps (2020).

[87]See Sec. 2.3 of Seeley (2018).

[88]We used the reference forward model (Dudhia, 2017) along with spectroscopic data from HiTRAN2016 (Gordon *et al.*, 2017).

[89]See Note 88.

[a]**Note:** This paper is part of the special issue on Teaching about the environment, sustainability, and climate change.

[b]ORCID: 0000-0002-6657-896X.

Allen, M. R., Friedlingstein, P., Girardin, C. A., Jenkins, S., Malhi, Y., Mitchell-Larson, E., Peters, G. P., and Rajamani, L., "Net zero: Science, origins, and implications," Annu. Rev. Environ. Resources **47**, 849–887 (2022).

Andrews, T., Gregory, J. M., and Webb, M. J., "The dependence of radiative forcing and feedback on evolving patterns of surface temperature change in climate models," J. Clim. **28**(4), 1630–1648 (2015).

Armour, K. C., "Energy budget constraints on climate sensitivity in light of inconstant climate feedbacks," Nat. Clim. Change **7**(5), 331–335 (2017).

Arrhenius, S., "On the influence of carbonic acid in the air upon the temperature of the ground," Philosoph. Mag. Ser. **41**(251), 237–276 (1896).

Bony, S., Stevens, B., Coppin, D., Becker, T., Reed, K. A., Voigt, A., and Medeiros, B., "Thermodynamic control of anvil cloud amount," Proc. Natl. Acad. Sci. U. S. A. **113**(32), 8927–8932 (2016).

Bretherton, C. S. and Wyant, M. C., "Moisture transport, lower-tropospheric stability, and decoupling of cloud-topped boundary layers," J. Atmos. Sci. **54**(1), 148–167 (1997).

Ceppi, P. and Nowack, P., "Observational evidence that cloud feedback amplifies global warming," Proc. Natl. Acad. Sci. U. S. A. **118**(30), e2026290118 (2021).
Charney, J., Arakawa, A., Baker, D. J., Bolin, B., Dickinson, R. E., Goody, R. M., Leith, C. E., Stommel, H. M., and Wunsch, C. I., "Carbon dioxide and climate: A scientific assessment," Technical report, National Academy of Sciences, Washington DC, 1979.
Coakley, Jr., J. A. and Yang, P., *Atmospheric Radiation: A Primer with Illustrative Solutions* (Wiley-VCH, New Jersey, 2014).
Colman, R. A., "Surface albedo feedbacks from climate variability and change," J. Geophys. Res. Atmos. **118**(7), 2827–2834, https://doi.org/10.1002/jgrd.50230 (2013).
Colman, R. and Soden, B. J., "Water vapor and lapse rate feedbacks in the climate system," Rev. Mod. Phys. **93**(4), 045002 (2021).
Cummins, D. P., Stephenson, D. B., and Stott, P. A., "Optimal estimation of stochastic energy balance model parameters," J. Clim. **33**(18), 7909–7926 (2020).
Donohoe, A., Armour, K. C., Pendergrass, A. G., and Battisti, D. S., "Shortwave and longwave radiative contributions to global warming under increasing CO_2," Proc. Natl. Acad. Sci. U. S. A. **111**(47), 16700–16705 (2014).
Dudhia, A., "The reference forward model (RFM)," J. Quant. Spectrosc. Radiative Transfer **186**, 243–253 (2017).
Emanuel, K., "The relevance of theory for contemporary research in atmospheres, oceans, and climate," AGU Adv. **1**(2), e2019AV000129 (2020).
Flynn, C. M. and Mauritsen, T., "On the climate sensitivity and historical warming evolution in recent coupled model ensembles," Atmos. Chem. Phys. **20**, 7829–7842 (2020).
Forster, P. M., Storelvmo, T., Armour, K., Collins, W., Dufresne, J. L., Frame, D., Lunt, D. J., Mauritsen, T., Palmer, M. D., Watanabe, M., Wild, M., and Zhang, H., "Chapter 7: The earth's energy budget, climate feedbacks, and climate sensitivity," *Climate Change 2021: The Physical Science Basis. Contribution of Working Group I to the Sixth Assessment Report of the Intergovernmental Panel on Climate Change*, Technical report, August, 2021.
Friedlingstein, P., O'Sullivan, M., Jones, M. W., Andrew, R. M., Hauck, J., Olsen, A., Peters, G. P., Peters, W., Pongratz, J., Sitch, S., Le Quéré, C., Canadell, J. G., Ciais, P., Jackson, R. B., Alin, S., Aragão, L. E., Arneth, A., Arora, V., Bates, N. R., Becker, M., Benoit-Cattin, A., Bittig, H. C., Bopp, L., Bultan, S., Chandra, N., Chevallier, F., Chini, L. P., Evans, W., Florentie, L., Forster, P. M., Gasser, T., Gehlen, M., Gilfillan, D., Gkritzalis, T., Gregor, L., Gruber, N., Harris, I., Hartung, K., Haverd, V., Houghton, R. A., Ilyina, T., Jain, A. K., Joetzjer, E., Kadono, K., Kato, E., Kitidis, V., Korsbakken, J. I., Landschützer, P., Lefèvre, N., Lenton, A., Lienert, S., Liu, Z., Lombardozzi, D., Marland, G., Metzl, N., Munro, D. R., Nabel, J. E., Nakaoka, S. I., Niwa, Y., O'Brien, K., Ono, T., Palmer, P. I., Pierrot, D., Poulter, B., Resplandy, L., Robertson, E., Rödenbeck, C., Schwinger, J., Séférian, R., Skjelvan, I., Smith, A. J., Sutton, A. J., Tanhua, T., Tans, P. P., Tian, H., Tilbrook, B., van Der Werf, G., Vuichard, N., Walker, A. P., Wanninkhof, R., Watson, A. J., Willis, D., Wiltshire, A. J., Yuan, W., Yue, X., and Zaehle, S., "Global carbon budget 2020," Earth Syst. Sci. Data **12**(4), 3269–3340 (2020).
Geoffroy, O., Saint-martin, D., Olivié, D. J., Voldoire, A., Bellon, G., and Tytéca, S., "Transient climate response in a two-layer energy-balance model. Part I: Analytical solution and parameter calibration using CMIP5 AOGCM experiments," J. Clim. **26**(6), 1841–1857 (2013).
Goodwin, P., Williams, R. G., Follows, M. J., and Dutkiewicz, S., "Ocean-atmosphere partitioning of anthropogenic carbon dioxide on centennial timescales," Global Biogeochemical Cycles **21**(1), 1–10 (2007).
Goodwin, P., Williams, R. G., and Ridgwell, A., "Sensitivity of climate to cumulative carbon emissions due to compensation of ocean heat and carbon uptake," Nat. Geosci. **8**(1), 29–34 (2015).
Gordon, I., Rothman, L., Hill, C., Kochanov, R., Tan, Y., Bernath, P., Birk, M., Boudon, V., Campargue, A., Chance, K., Drouin, B., Flaud, J.-M., Gamache, R., Hodges, J., Jacquemart, D., Perevalov, V., Perrin, A., Shine, K., Smith, M.-A., Tennyson, J., Toon, G., Tran, H., Tyuterev, V., Barbe, A., Császár, A., Devi, V., Furtenbacher, T., Harrison, J., Hartmann, J.-M., Jolly, A., Johnson, T., Karman, T., Kleiner, I., Kyuberis, A., Loos, J., Lyulin, O., Massie, S., Mikhailenko, S., Moazzen-Ahmadi, N., Müller, H., Naumenko, O., Nikitin, A., Polyansky, O., Rey, M., Rotger, M., Sharpe, S., Sung, K., Starikova, E., Tashkun, S., Auwera, J. V., Wagner, G., Wilzewski, J., Wcisło, P., Yu, S., and Zak, E., "The HITRAN2016 molecular spectroscopic database," J. Quant. Spectrosc. Radiative Transfer **203**, 3–69 (2017).
Gregory, J. M., "Vertical heat transports in the ocean and their effect on time-dependent climate change," Clim. Dyn. **16**(7), 501–515 (2000).
Hall, A., "The role of surface albedo feedback in climate," J. Clim. **17**(7), 1550–1568 (2004).
Hansen, J., "Climate sensitivity: Analysis of feedback mechanisms," Geophys. Monograph **29**(5), 1 (1984).
Hansen, J., Johnson, D., Lacis, A., Lebedeff, S., Lee, P., Rind, D., and Russell, G., "Climate impact of increasing atmospheric carbon dioxide," Science **213**(4511), 957–966 (1981).
Hansen, J., Sato, M., and Ruedy, R., "Radiative forcing and climate response," J. Geophys. Res. Atmos. **102**(D6), 6831–6864, https://doi.org/10.1029/96JD03436 (1997).
Hartmann, D. L., *Global Physical Climatology*, 2nd ed. (Elsevier Science, 2015).
Hartmann, D. L. and Larson, K., "An important constraint on tropical cloud - climate feedback," Geophysical Res. Lett. **29**(20), 12-1–12-4 (2002).
He, H., Kramer, R. J., Soden, B. J., and Jeevanjee, N., "State-dependence of CO_2 forcing and its implications for climate sensitivity," arXiv:2210.12244 (2022).
Held, I. M. and Soden, B. J., "Robust responses of the hydrological cycle to global warming," J. Clim. **19**, 5686–5699 (2006).
Held, I. M., Winton, M., Takahashi, K., Delworth, T., Zeng, F., and Vallis, G. K., "Probing the fast and slow components of global warming by returning abruptly to preindustrial forcing," J. Clim. **23**(9), 2418–2427 (2010).
Climate Change 1994: Radiative Forcing of Climate Change and an Evaluation of the IPCC 1992 IS92 Emission Scenarios, edited by J. T. Houghton, L. Meira Filho, J. Bruce, H. Lee, B. Callander, E. Haites, N. Harris, and K. Maskell(Cambridge U. P., Cambridge, 1994).
Huang, Y., Tan, X., and Xia, Y., "Inhomogeneous radiative forcing of homogeneous greenhouse gases," J. Geophysical Res. **121**(6), 2780–2789 (2016).
Ingram, W. J., "A very simple model for the water vapour feedback on climate change," Q. J. R. Meteorological Soc. **136**(646), 30–40 (2010).
Jeevanjee, N., "The physics of climate change: Simple models in climate science," arXiv:1804.09326 (2018).
Jeevanjee, N. and Fueglistaler, S., "On the cooling-to-space approximation," J. Atmos. Sci. **77**(2), 465–478 (2020a).
Jeevanjee, N. and Fueglistaler, S., "Simple spectral models for atmospheric radiative cooling," J. Atmos. Sci. **77**(2), 479–497 (2020b).
Jeevanjee, N., Held, I., and Ramaswamy, V., "Manabe's radiative-convective equilibrium," Bull. Am. Meteorological Soc. **103**(11), E2533–E2543 (2022).
Jeevanjee, N., Koll, D. D. B., and Lutsko, N. J., "'Simpson's law' and the spectral cancellation of climate feedbacks," Geophysical Res. Lett. **48**(14), e2021GL093699 (2021a).
Jeevanjee, N., Seeley, J. T., Paynter, D., and Fueglistaler, S., "An analytical model for spatially varying clear-sky CO_2 forcing," J. Clim. **34**(23), 9463–9480 (2021b).
Klein, S. A., Hall, A., Norris, J. R., and Pincus, R., "Low-cloud feedbacks from cloud-controlling factors: A review," Surv. Geophys. **38**(6), 1307–1329 (2017).
Koll, D. D. B. and Cronin, T. W., "Earth's outgoing longwave radiation linear due to H_2O greenhouse effect," Proc. Natl. Acad. Sci. U. S. A. **115**(41), 10293–10298 (2018).
Koll, D. D. B., Jeevanjee, N., and Lutsko, N. J., "An analytical model for the clear-sky longwave feedback," (published online, 2022).
Leach, N. J., Jenkins, S., Nicholls, Z., Smith, C. J., Lynch, J., Cain, M., Walsh, T., Wu, B., Tsutsui, J., and Allen, M. R., "FaIRv2.0.0: A generalized impulse response model for climate uncertainty and future scenario exploration," Geoscientific Model Develop. **14**(5), 3007–3036 (2021).
Lilly, D., "Models of cloud-topped mixed layers under a strong inversion," Q. J. R. Meteorological Soc. **94**, 292–309 (1968).
MacDougall, A. H., "The transient response to cumulative CO_2 emissions: A review," Curr. Clim. Change Rep. **2**(1), 39–47 (2016).
MacDougall, A. H. and Friedlingstein, P., "The origin and limits of the near proportionality between climate warming and cumulative CO_2 emissions," J. Clim. **28**(10), 4217–4230 (2015).
MacDougall, A. H., Frölicher, T. L., Jones, C. D., Rogelj, J., DamonMatthews, H., Zickfeld, K., Arora, V. K., Barrett, N. J., Brovkin, V., Burger, F. A., Eby, M., Eliseev, A. V., Hajima, T., Holden, P. B., Jeltsch-Thömmes, A., Koven, C., Mengis, N., Menviel, L., Michou, M., Mokhov, I. I., Oka, A., Schwinger, J., Séférian, R., Shaffer, G., Sokolov, A., Tachiiri, K., Tjiputra, J., Wiltshire, A., and Ziehn, T., "Is there

warming in the pipeline? A multi-model analysis of the zero emissions commitment from CO_2," Biogeosciences **17**(11), 2987–3016 (2020).
Manabe, S. and Strickler, R. F., "Thermal equilibrium of the atmosphere with a convective adjustment," J. Atmos. Sci. **21**(4), 361–385 (1964).
Manabe, S. and Wetherald, R. T., "Thermal equilibrium of the atmosphere with a given distribution of relative humidity," J. Atmos. Sci. **24**(3), 241–259 (1967).
Marshall, D. P. and Zanna, L., "A conceptual model of ocean heat uptake under climate change," J. Clim. **27**(22), 8444–8465 (2014).
Mauritsen, T. and Stevens, B., "Missing iris effect as a possible cause of muted hydrological change and high climate sensitivity in models," Nat. Geosci. **8**(5), 346–351 (2015).
McKim, B. A., Bony, S., and Dufresne, J.-L. (2023). Physical and observational constraints on the anvil cloud feedback. ESSOAR Preprint, available at https://essopenarchive.org/users/538471/articles/627002-physical-and-observational.
McKim, B. A., Jeevanjee, N., and Vallis, G. K., "Joint dependence of longwave feedback on surface temperature and relative humidity," Geophysical Res. Lett. **48**(18), e2021GL094074 (2021).
Meehl, G. A., Senior, C. A., Eyring, V., Flato, G., Lamarque, J. F., Stouffer, R. J., Taylor, K. E., and Schlund, M., "Context for interpreting equilibrium climate sensitivity and transient climate response from the CMIP6 Earth system models," Sci. Adv. **6**(26), 1–11 (2020).
Meinshausen, M., Raper, S. C., and Wigley, T. M., "Emulating coupled atmosphere-ocean and carbon cycle models with a simpler model, MAGICC6 - Part 1: Model description and calibration," Atmos. Chem. Phys. **11**(4), 1417–1456 (2011).
Myers, T. A., Scott, R. C., Zelinka, M. D., Klein, S. A., Norris, J. R., and Caldwell, P. M., "Observational constraints on low cloud feedback reduce uncertainty of climate sensitivity," Nat. Clim. Change **11**(6), 501–507 (2021).
Myhre, G., Highwood, E. J., Shine, K. P., and Stordal, F., "New estimates of radiative forcing due to well mixed greenhouse gases," Geophysical Res. Lett. **25**(14), 2715–2718 (1998).
North, G. R., Cahalan, R. F., and Coakley, J. A., "Energy balance climate models," Rev. Geophys. **19**(1), 91–121, https://doi.org/10.1029/RG019i001p00091 (1981).
Payne, A. E., Jansen, M. F., and Cronin, T. W., "Conceptual model analysis of the influence of temperature feedbacks on polar amplification," Geophysical Res. Lett. **42**(21), 9561–9570 (2015).
Petty, G. W., *A First Course in Atmospheric Radiation*, 2nd ed. (Sundog Pub., Wisconsin, 2006).
Pierrehumbert, R. T., *Principles of Planetary Climate* (Cambridge U. P., Cambridge, 2010).
Pierrehumbert, R. T., "Infrared radiative and planetary temperature," Phys. Today **64**(1), 33–38 (2011).
Proistosescu, C. and Huybers, P. J., "Slow climate mode reconciles historical and model-based estimates of climate sensitivity," Sci. Adv. **3**(7), 1–7 (2017).
Ramaswamy, V., Collins, W., Haywood, J., Lean, J., Mahowald, N., Myhre, G., Naik, V., Shine, K. P., Soden, B., Stenchikov, G., and Storelvmo, T., "Radiative forcing of climate: The historical evolution of the radiative forcing concept, the forcing agents and their quantification, and applications," Meteorol. Monographs **59**, 14.1–14.101 (2019).
Randall, D. A., *Atmosphere, Clouds, and Climate* (Princeton U. P., Princeton, 2012).
Romps, D. M., "Theory of tropical moist convectionà," in *Fundamental Aspects of Turbulent ßows in Climate Dynamicsà*, edited by F. Bouchet, T. Schneider, A. Venaille, C. Salomon (Oxford University Press, 2020).
Romps, D. M., Seeley, J. T., and Edman, J. P., "Why the forcing from carbon dioxide scales as the logarithm of its concentration," J. Clim. **35**(13), 4027–4047 (2022).
Schneider, S. H. and Thomspon, S. L., "Atmospheric CO_2 and climate: Importance of the transient response," J. Geophysical Res. **86**(C4), 3135–3147 (1981).
Seeley, J. T., "Convection, radiation, and climate: fundamental mechanisms and impacts of a changing atmosphere," PhD thesis, University of California Berkeley, 2018).
Seeley, J. T., Jeevanjee, N., and Romps, D. M., "FAT or FiTT: Are anvil clouds or the tropopause temperature invariant?," Geophysical Res. Lett. **46**(3), 1842–1850 (2019).
Seshadri, A. K., "Origin of path independence between cumulative CO_2 emissions and global warming," Clim. Dyn. **49**(9–10), 3383–3401 (2017).
Sherwood, S. C., Bony, S., Boucher, O., Bretherton, C. S., Forster, P. M., Gregory, J. M., and Stevens, B., "Adjustments in the forcing-feedback framework for understanding climate change," Bull. Am. Meteorological Soc. **96**(2), 217–228 (2015).
Sherwood, S. C., Webb, M. J., Annan, J. D., Armour, K. C., Forster, P. M., Hargreaves, J. C., Hegerl, G., Klein, S. A., Marvel, K. D., Rohling, E. J., Watanabe, M., Andrews, T., Braconnot, P., Bretherton, C. S., Foster, G. L., Hausfather, Z., Heydt, A. S., Knutti, R., Mauritsen, T., Norris, J. R., Proistosescu, C., Rugenstein, M., Schmidt, G. A., Tokarska, K. B., and Zelinka, M. D., "An assessment of earth's climate sensitivity using multiple lines of evidence," Rev. Geophys. **58**(4), e2019RG000678, https://doi.org/10.1029/2019RG000678 (2020).
Shine, K. P., Ptashnik, I. V., and Rädel, G., "The water vapour continuum: Brief history and recent developments," Surv. Geophys. **33**(3–4), 535–555 (2012).
Siebesma, A. P., Bony, S., Jakob, C., and Stevens, B., *Clouds and Climate: Climate Science's Greatest Challenge* (Cambridge U. P., Cambridge, 2020).
Siegenthaler, U. and Oeschger, H., "Transient temperature changes due to increasing CO_2 using simple models," Ann. Glaciology **5**, 153–159 (1984).
Simpson, G., "Some studies in terrestrial radiation," Memoirs R. Meteorological Soc. **2**(16), 69–95 (1928).
Stephens, G. L., O'Brien, D., Webster, P. J., Pilewski, P., Kato, S., and Li, J.-L., "The albedo of earth," Rev. Geophys. **53**(1), 141–163, https://doi.org/10.1002/2014RG000449 (2015).
Stevens, B. and Kluft, L., "A colorful look at climate sensitivity," *EGUsphere* (2023) pp. 1–24.
Tarshish, N., Jeevanjee, N., and Fung, I., "Constraining the post-emissions temperature change,"<https://www.researchsquare.com/article/rs-1519965/v1>, 2022.
Thompson, D. W. J., Bony, S., and Li, Y., "Thermodynamic constraint on the depth of the global tropospheric circulation," Proc. Natl. Acad. Sci. **114**(31), 8181–8186 (2017).
Trenberth, K. E. and Fasullo, J. T., "Global warming due to increasing absorbed solar radiation," Geophysical Res. Lett. **36**(7), 1–5 (2009).
Tsutsui, J., "Diagnosing transient response to CO_2 forcing in coupled atmosphere-ocean model experiments using a climate model emulator," Geophysical Res. Lett. **47**(7), e2019GL085844 (2020).
Tziperman, E., *Global Warming Science: A Quantitative Introduction to Climate Change and Its Consequences* (Princeton U. P., Princeton, 2022).
Vallis, G. K., *Climate and the Oceans* (Princeton U. P., Princeton, 2012).
Wallace, J. M. and Hobbs, P. V., *Atmospheric Science: An Introductory Survey* (Academic Press, Cambridge, 2006).
Wigley, T. M. L. and Schlesinger, M. E., "Analytical solution for the effect of increasing CO_2 on global mean temperature," Nature **315**(6021), 649–652 (1985).
Wilson, D. J. and Gea-Banacloche, J., "Simple model to estimate the contribution of atmospheric CO_2 to the earth's greenhouse effect," Am. J. Phys. **80**(4), 306–315 (2012).
Zelinka, M. D., Myers, T. A., McCoy, D. T., Po-Chedley, S., Caldwell, P. M., Ceppi, P., Klein, S. A., and Taylor, K. E., "Causes of higher climate sensitivity in CMIP6 models," Geophysical Res. Lett. **47**(1), e2019GL085782 (2020).
Zelinka, M. D., Zhou, C., and Klein, S. A., "Insights from a refined decomposition of cloud feedbacks," Geophysical Res. Lett. **43**(17), 9259–9269 (2016).
Zhang, Y., Jeevanjee, N., and Fueglistaler, S., "Linearity of outgoing longwave radiation: From an atmospheric column to global climate models," Geophysical Res. Lett. **47**(17), e2020GL089235 (2020).